Investigation of Germination and Aging in Moravian III Barley Grain by Nuclear Magnetic Resonance

Cynthia F. Ridenour, Jincheng Xiong, and Gary E. Maciel
Department of Chemistry, Colorado State University, Fort Collins, Colorado 80523 USA

ABSTRACT High-resolution, solid-state ^{1}H nuclear magnetic resonance (NMR) techniques are used for the first time to study germination in imbibed Moravian III barley grains. Whereas magic-angle spinning ^{1}H NMR spectra reveal the water and lipid components in barley grains, combined rotation and multiple-pulse spectroscopy techniques provide ^{1}H NMR spectra of grains that reveal the protein and carbohydrate as well as the water and lipid components. Spectra of grains are compared with spectra of model compounds to verify assignments. ^{1}H T_1 and T_2 measurements using magic-angle spinning only and combined rotation and multiple-pulse spectroscopy techniques provide information about molecular mobility within the grains during imbibition. Some grains were subjected to artificial aging conditions. ^{1}H NMR spectral comparisons are made between normal, viable grains and artificially aged grains.

INTRODUCTION

Nuclear magnetic resonance (NMR) has become one of the most widely used techniques for analysis of molecular structure and dynamics (Farrar and Becker, 1971; Bovey et al., 1987; Derome, 1987; Bovey, 1988). Applications to liquid samples are far more numerous than solid-state applications. Dormant and imbibed seeds are relatively solid-like or semisolid biological tissues, and information obtained by liquid-type NMR experiments performed on intact seeds is limited to detection of mobile water, dissolved sugars, mobile lipid, and mobilized phosphate species (Conway and Smith, 1962; Schaefer and Stejskal, 1974; Colnago and Seidl, 1983; Tomassetti et al., 1986).

^{1}H NMR spectra have previously been obtained on single sunflower and black turtle bean seeds (Rutar, 1989) by the magic-angle spinning (MAS) technique (Lowe, 1959; Kessemeier and Norberg, 1967; Andrew et al., 1969) to narrow lines. ^{1}H resonances of highly mobile lipid and water were observed in the spectra obtained by this method, as MAS is capable of averaging ^{1}H chemical shift anisotropies, heteronuclear magnetic dipole–dipole interactions and weak ^{1}H–^{1}H magnetic dipole–dipole interactions (e.g., of relatively mobile species). However, high-resolution ^{1}H NMR spectra of rigid solids are more difficult to obtain, because the homonuclear ^{1}H–^{1}H dipolar couplings can contribute line broadening of more than 10^4 Hz. For solid materials rich in protons in rigid structures, an adequate spinning speed has not yet been achieved. If reliable high-resolution NMR observation of protons is desired, then a class of experiments called combined rotation and multiple-pulse spectroscopy (CRAMPS) can be used to achieve high-resolution ^{1}H NMR spectra of rigid solids (Gerstein et al., 1977; Bronnimann et al., 1988; Maciel et al., 1990). In these experiments, MAS averages proton chemical shift anisotropy, and an appropriate multiple-pulse cycle averages the homonuclear dipolar interaction. Until recently, the CRAMPS technique has not been widely implemented. To our knowledge, the CRAMPS results presented here are the only high-resolution solid-state ^{1}H NMR spectra that have yet been obtained on seeds by the CRAMPS technique.

Results presented here follow Moravian III barley grain germination noninvasively by ^{1}H NMR. Two methods of line narrowing were utilized and are contrasted in this paper: MAS with spin excitation by a single pulse (SP/MAS) and CRAMPS. ^{1}H T_1 and T_2 data are presented that reveal dynamical information about the states of water, lipid membranes, and storage reserves during imbibition. Both viable and artificially aged barley grains have been investigated by ^{1}H NMR, and the results for fresh and aged grains are compared. These results lead to a hypothesis about the aging process in the barley grains investigated in this study. It is also shown that the grains can withstand the sample spinning and radio-frequency power levels applied during CRAMPS analysis to remain viable and vigorous for subsequent germination and growth.

MATERIALS AND METHODS

Amylopectin and γ-globulin were obtained from the Sigma Chemical Company (St. Louis, MO). The coconut oil used was obtained from a local grocery store. Barley grain (*Hordeum vulgare*, cv. Moravian III) used in this study was supplied by the Adolph Coors Company (Golden, CO). Grains were stored under controlled environmental conditions at 33% relative humidity (RH) and room temperature. Accelerated aging was accomplished by subjecting some of the grains to conditions of 40°C and either 0% RH (relative humidity) or 100% RH for 11 or 26 days. The artificially aged grains were then returned to normal controlled storage (33% RH and room temperature) until the NMR experiments were performed. The degree of germination determined for the barley stored under normal conditions and for the barley aged under 0% RH was close to

Received for publication 1 November 1993 and in final form 12 October 1995

Address reprint requests to Dr. Gary E. Maciel, Department of Chemistry, Colorado State University, Fort Collins, CO 80523-0002. Tel.: 970-491-6480; Fax: 970-491-1801; E-mail: maciel@lamar.colostate.edu. Dr. Redenour's current address: Otsuka Electronics, Inc., 2555 Midpoint Drive, Fort Collins, CO 80525.

© 1996 by the Biophysical Society

0006-3495/96/01/511/21 $2.00

100%, whereas the degree of germination of the barley aged under 100% RH was close to 0%, as determined by a standard ISTA germination assay procedure (International Seed Testing Assocation, 1976). In this procedure, barley grain is imbibed in moistened paper towel rolls and the number and vigor of germinated grains is assessed after several days of imbibition.

We performed vigor tests to determine the deleterious effect, if any, of the experimental conditions of the CRAMPS technique on the viability and vigor of the barley grain. At issue was whether the spinning rates and high-radio-frequency power used in CRAMPS experiments destroyed the tissue during analysis. A good indicator of seed-tissue integrity is seedling vigor. To determine the relative vigor of barley following NMR analysis, we performed a standard germination assay, but during the assay, we interrupted imbibition by some grains to perform CRAMPS experiments. Following the CRAMPS analysis, the grains were returned to the imbibition chamber. Vigor was determined after several days of seedling growth in the imbibition chamber, and comparison of the growth of the NMR-analyzed grains with the growth of control grains was made.

Twenty grains were used as a control set, and the test set comprised seven grains that were subjected to CRAMPS analysis. The control set experienced continuous imbibition and no NMR analysis. The test grains were removed from the germination chamber after 17–19 h of imbibition for ^{1}H CRAMPS analysis of approximately 20–30-min duration per grain. Following the NMR experiments, the test grains were put back into the germination chamber after ~2 h out of the chamber. At the end of 88 h of imbibition, the lengths of the shoots and roots of the control seedlings were measured. After 88 h, plus 2.25 h of time during which the grains were out of the germination chamber, the shoot lengths and root lengths of the test seedlings were measured. The results of the vigor tests are shown in Table 1. As seen from the table, grains remained vigorous after being subjected to the NMR analysis under the conditions described below, and growth was normal compared with that in the control set. Analogous experiments at higher MAS speeds showed that spinning rates greater than 2.0 kHz cannot be employed without destroying germinated barley. Unimbibed grains can easily withstand moderate spinning speeds (perhaps up to 5 kHz), whereas seedlings with several days' growth are very intolerant of MAS at any speed significant for averaging strong dipolar interactions. Hence, fast MAS is not a suitable alternative to CRAMPS for ^{1}H NMR experiments on germinating or germinated seeds.

We accomplished imbibition of grain for NMR analysis, aside from the vigor test and the germination assays, by placing the barley grains on moistened blotter paper in a germination chamber. The barley grains all began imbibition after storage at 33% RH and initially contained 8.6% water by weight, as determined by weight loss during oven drying. We removed grain from controlled storage and weighed it before imbibition and then again after imbibition, before the NMR experiments, to determine the increase in fresh weight of the grain during imbibition. Assuming that all the increase in fresh weight during imbibition is due to water uptake, we calculated the percent water in the imbibed grains. In this calculation, to the weight gained during imbibition one adds 8.6% of the preimbibition weight and divides by the postimbibition weight, to find the percent water in the imbibed grain.

All ^{1}H NMR experiments were performed on single intact grains or, in a limited number of experiments, on small numbers of excised embryos, with a severely modified Nicolet NT-200 NMR instrument operating at 187 MHz and a severely modified NT-360 instrument operating at 360 MHz. Most of the data acquired in this study were obtained at 187 MHz; the use of 360 MHz is specifically indicated where appropriate. MAS speeds were 1.0–1.5 kHz. The multiple-pulse sequence used for ^{1}H CRAMPS detection was BR-24 (Burum and Rhim, 1979), with a 108-μs cycle time and a $\pi/2$ pulse width of 1.1–1.3 μs. Data array sizes were 256-1024 points and recycle delays were 5–10 s for CRAMPS detection and 3–10 s for SP/MAS experiments (excitation by a single 90° pulse). The number of scans that were acquired per spectrum ranged from 24 to 120. ^{1}H relaxation times (T_1 and T_2) were measured with the SP/MAS and CRAMPS versions (Bronnimann et al., 1988) of the Freeman–Hill (1971) approach and the Hahn (1950) spin-echo experiment, respectively. The dephasing periods (and corresponding pulses) in the Hahn spin-echo experiments were synchronized to the rotor to prevent dipolar echo effects in experiments with longer dephasing periods.

TABLE 1 Barley grain germination* test results for untreated barley grains (MIII), artificially aged barley grains, ‡control grains, and barley grains subjected to ^{1}H CRAMPS NMR experimental conditions during imbibition§

	No. of Grains	Water Content¶	Germination Success	Root Length (cm)		Shoot Length (cm)	
				Mean	SD	Mean	SD
MIII	15	80%	100%	8.7	0.7	3.0	0.6
M-D-11‡,‖	15	79%	93%	9.4	0.8	2.9	0.5
M-D-26‡,**	15	80%	100%	8.9	1.0	2.9	0.7
M-W-11‡,§§	15	42%	0%	–	–	–	–
M-W-26‡,‖‖	15	43%	0%	–	–	–	–
Control	20		100%	10.7	0.9	3.8	0.5
Test Seeds§	7		100%	9.6	1.3	4.0	0.4

*The germination assays were carried out simultaneously over a period of 91–92 h.
¶Water content is on a fresh weight basis following imbibition.
‖Grain aged under conditions of 0% RH and 40°C for 11 days.
**Grain aged under conditions of 0% RH and 40°C for 26 days.
§§Grain aged under conditions of 100% RH and 40°C for 11 days.
‖‖Grain aged under conditions of 100% RH and 40°C for 26 days.

RESULTS AND DISCUSSION

^{1}H NMR spectra of barley grains

SP/static, MP/static, SP/MAS, and CRAMPS

As indicated in the Introduction, ^{1}H NMR spectra of rigid, solid materials can be very broad, more than 10^4 kHz, unless line-narrowing techniques such as the multiple-pulse (MP) method are employed. When the sample under consideration is a complex system such as a seed, some components within the sample may be contained in a very rigid environment, whereas other components may be more mobile. The more liquidlike environment consists of inherently mobile lipids and water in a dormant seed as well as hydrated regions in an imbibed seed. The ^{1}H NMR spectra of a single, fresh, unimbibed, intact Moravian III barley grain have been obtained by SP/static, MP/static (multiple pulse, no spinning), SP/MAS, and CRAMPS (MP/MAS) methods and are shown in Fig. 1.

The SP/static ^{1}H NMR spectrum of a quiescent barley grain, obtained with no line-narrowing procedure, is shown in Fig. 1 (*a*). The SP/static ^{1}H experiment utilizes a single 90° radio-frequency pulse, followed by detection of the (Bloch-decay) signal. No form of line narrowing is applied. Only two broad, poorly resolved features are observed in the spectrum. On the basis of work done with model compounds and known chemical shifts (Conway and Johnson, 1969), the SP/static ^{1}H NMR peak centered at ~1 ppm can be identified with lipid resonances and the peak at ~5 ppm can be attributed to water. Although lipids are highly mobile, the motion is anisotropic and is mostly restricted to fast rotation about the long axis of the molecule (Voet and Voet, 1990). Hence, motional narrowing is incomplete. The SP/

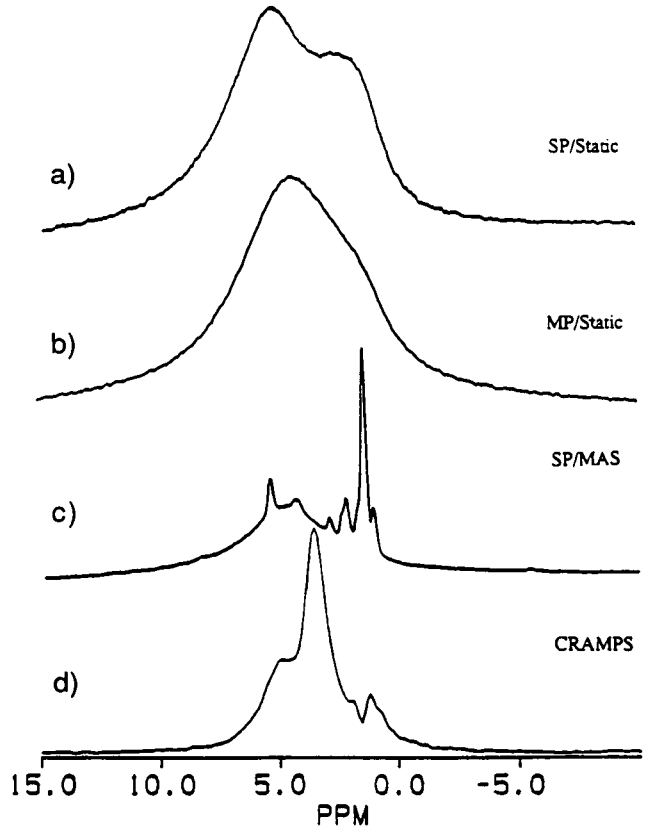

FIGURE 1 ^{1}H NMR spectra of a barley grain with arbitrary vertical scaling. The spectra were acquired on a single, intact Moravian III barley grain at 187 MHz. Recycle delay, 5 s; spinning speed in (*c*) and (*d*) ~1.5 kHz; BR-24 pulse sequence used for (*d*) with a 3-μs τ value.

static ^{1}H NMR spectrum of lipids in seeds shows broad lines resulting from residual chemical shift anisotropy broadening, distributions of isotropic chemical shifts, residual ^{1}H–^{1}H dipolar broadening, and magnetic susceptibility differences across the sample (Conway and Johnson, 1969; O'Donnell et al., 1981). The breadth of the water peak results from a combination of chemical shift anisotropy and dipolar interactions manifested because of restricted motion of bound water and of the chemical shift dispersion of water molecules residing in a variety of different environments, e.g., hydrogen bonding structures and macromolecular hydration sites. As Fig. 1 (*a*) is a spectrum of a quiescent, umimbibed grain, most of the water present is believed to be tightly bound in strong hydration sites (Priestley, 1986). The ^{1}H NMR peaks of carbohydrate and protein constituents of a quiescent seed are tens of kilohertz broad in a SP/static spectrum.

Fig. 1 (*b*) shows the ^{1}H NMR spectrum of the quiescent barley grain obtained by BR-24 MP line narrowing but without MAS (MP/static). A peak is observed that is relatively featureless. Superficially, this spectrum would seem to contain less information than the one of Fig. 1 (*a*) that is acquired without any line-narrowing procedure. However, the ^{1}H spectrum of Fig. 1 (*b*) contains discernible (broad) contributions from protein and carbohydrate molecules within the barley grain, whereas the spectrum of Fig. 1 (*a*) does not (too broad). MP line narrowing eliminates homonuclear dipole–dipole broadening in Fig. 1 (*b*), but chemical shift anisotropy broadening, isotropic chemical shift dispersion, and variation of magnetic susceptibility across the sample are still manifested, so the resulting spectrum does not offer crisp resolution of peaks arising from individual chemical sites.

The spectrum in Fig. 1 (*c*) is a ^{1}H NMR spectrum of the same grain acquired with the SP/MAS technique, which employs only MAS for line narrowing. Individual lipid proton resonances are resolved and can be assigned (Rutar, 1989), but the intensity that is due to contributions from protons experiencing strong ^{1}H–^{1}H dipolar interactions is spread out along the baseline and is not readily discernible. The peak at 0.9 ppm represents terminal CH_3 protons (three protons for every fatty acid chain); the 1.3-ppm peak arises from CH_2 protons in the interior of methylene chains; peaks at 2.3 and 1.7 ppm are due to protons in fatty acid methylene chains that are α and β, respectively, to ester linkages to glycerol moieties. The 2.0-ppm peak arises from methylene protons adjacent to one vinyl group, and the 2.8-ppm peak represents methylene protons in C=CHCH$_2$CH=C structures. The ^{1}H NMR peaks of glyceride protons appear at 4.1, 4.3, and 5.3 ppm. The glyceride methine proton resonance at 5.3 ppm is overlapped by the more abundant vinyl proton resonances in the spectrum of Fig. 1 (*c*). Peaks at 2.0, 2.8, and 5.3 ppm are useful for monitoring the degree of unsaturation, because they correspond to protons on or near sp^2 carbons.

The MAS speed employed in obtaining the spectrum shown in Fig. 1 (*c*) is sufficient to average the chemical shift and magnetic susceptibility anisotropy of the lipid protons and thus produces narrow lines. Dipolar couplings between lipid protons are attenuated because of the rapid rotation of the methylene chains about the long axis. The water peak at ~4.7 ppm in Fig. 1 (*c*) is still broad, probably because of a combination of isotropic chemical shift dispersion (i.e., a range of hydrogen-bonding environments) and proton–proton dipolar interactions within the strongly bound water molecules and/or between water protons and hydrated substrate protons. In the SP/MAS ^{1}H NMR technique the MAS rate that would be required effectively to eliminate line broadening resulting from ^{1}H–^{1}H dipolar interactions in rigid molecules in the grain would destroy the grain.

The ^{1}H CRAMPS spectrum of the barley grain is shown in Fig. 1 (*d*). All protons in the grain should contribute to the CRAMPS spectrum. An "average" barley grain contains 76% carbohydrate, 12% protein, and 3% lipids (Bewley and Black, 1985), so the ^{1}H CRAMPS spectrum shown in Fig. 1 (*d*) is dominated by the starch methylene peak at 3.7 ppm and the starch hydroxyl peak at 5.1 ppm. The most prominent lipid peak, which appears at 1.3 ppm in the SP/MAS spectrum, can be seen in the CRAMPS spectrum and is overlapped by aliphatic protein resonances that also appear in that region of the spectrum. Other lipid, protein, and

water resonances are unresolved from the starch peaks that dominate the barley spectrum in Fig. 1 (*d*).

Lipid peaks are broader in the CRAMPS spectrum than in the SP/MAS spectrum. Although, in principle, some of this line broadening can be attributed to imperfections in the MP train of the CRAMPS experiment, our experience is that this effect contributes less than ~0.2 ppm to the linewidth currently achievable by MP techniques. ^{1}H lines arising from liquids are typically broadened in a CRAMPS spectrum, relative to a SP/MAS spectrum. For example, cyclohexane has a ^{1}H SP/MAS linewidth of 6.5 Hz at 187 MHz and a ^{1}H CRAMPS linewidth of 30 Hz. Pure coconut oil has an observed ^{1}H SP/MAS linewidth of 19 Hz and a ^{1}H CRAMPS linewidth of 40 Hz. Some broadening of the lipid lines in the CRAMPS spectrum relative to the SP/MAS spectrum may also result from motion in the lipid molecules with frequencies comparable with the inverse of the MP cycle time. Motions at these frequencies interfere with the averaging of the ^{1}H–^{1}H dipolar Hamiltonian by the MP sequence (Wittebort et al., 1988). This line-broadening mechanism for lipid peaks in the CRAMPS spectrum presupposes that there are significant numbers of protons contained in lipids of the barley grain that maintain substantial dipolar couplings and do not contribute to the SP/MAS spectrum of the barley grain. CRAMPS experiments performed on barley grains at different temperatures would perhaps illuminate this linewidth issue.

The ^{1}H spectra shown in Fig. 1, and the discussion above, imply that the ^{1}H CRAMPS spectra display all, or at least most, of the hydrogen in the quiescent barley seed, whereas the SP/MAS spectra display only the most mobile components. To examine and test this interpretation, we carried out a series of experiments designed to count the number of spins detected in ^{1}H CRAMPS and SP/MAS experiments on an individual quiescent barley seed. For this purpose, the proton NMR signal of a small, weighed quantity of silicone rubber, $[(CH_3)_2Si\text{-}O\text{-}]_n$, added to the seed in the MAS rotor, was used as an internal intensity reference. For a specific sample, the CRAMPS spectrum manifested an 11.2 ratio of the intensity of the seed signals to that of the silicone rubber signals, whereas the corresponding ratio in the SP/MAS spectrum was only 0.86. Hence, only a small fraction, less than roughly 8%, of the ^{1}H NMR intensity observed for a seed in the CRAMPS experiment is seen in the SP/MAS experiment. A priori, these ratios could be explained if, for some reason (e.g., motional interference with the MP line narrowing), the CRAMPS technique discriminated against the silicone rubber magnetization. However, in calibration experiments for the CRAMPS version of this "spin-counting" strategy, weighed physical mixtures of silicone rubber with powdered monoethylfumarate yielded the correct intensity ratios for the two components within ±5%; similar calibration experiments with weighed mixtures of silicone rubber and adamantane yielded results that correspond within 5% to the value predicted from the sample weights and chemical formulas. Analogous adamantane calibration experiments with the MAS-only method yield results within 3% of the correct values. Hence, the huge discrepancy between the fractions of protons observed for a seed in CRAMPS and SP/MAS experiments *cannot* be explained on the basis of discrimination against the silicone rubber signal in the CRAMPS experiment. Of course, the size of the CRAMPS-over-SP/MAS dominance in the fraction of protons detected will depend on the state of the seed; e.g., one expects it to be smaller in a germinating seed, in which a larger fraction of the protons are in mobile moieties (e.g., water).

Major molecular contributions to barley-grain CRAMPS spectrum

One can simulate the ^{1}H CRAMPS spectrum of barley by adding together CRAMPS spectra of three model systems. Results of such a simulation are shown in Fig. 2. CRAMPS spectra of amylopectin, γ-globulin, and coconut oil, respectively, are shown in Fig. 2 (*c*)–(*e*). These samples were chosen to represent the three types of molecule that constitute most of a barley grain: carbohydrate, protein, and lipid. For the simulation, the spectral contributions of these model compounds were scaled according to the fraction of the represented constituent contained in a typical barley grain and then added together to produce the "simulated" barley spectrum shown in Fig. 2 (*b*). It should be noted perhaps that overlaps, which are due to more than one component in the 1.3-ppm peak and more than one in the 3.7-ppm peak, render it difficult, if not impossible, to use these peaks for quantitative compositional analysis.

CRAMPS and SP/MAS spectra of untreated and aged grains

Moravian III barley grains were aged artificially and studied with solid-state ^{1}H NMR techniques. Aging conditions were

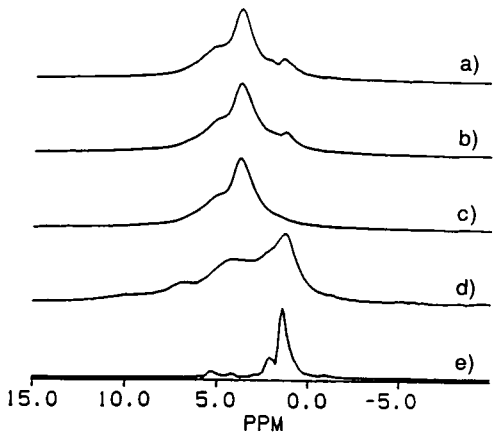

FIGURE 2 Construction of the ^{1}H CRAMPS spectrum of Moravian III barley grain from spectra of major constituents of the grain. (*a*) Moravian III barley grain spectrum; (*b*) spectrum constructed from coaddition of (*c*)–(*e*), with each contributing spectrum scaled according to the relative contribution of the represented nutrient to the total barley seed; (*c*) amylopectin spectrum, representing the starch fraction; (*d*) γ-globulin spectrum representing protein; (*e*) coconut oil spectrum representing lipid. All spectra were acquired by use of the BR-24 pulse sequence at 187 MHz, with a 1–2 kHz MAS speed.

0% RH and 100% RH at 40°C for 11 and 26 days. The dry-aged grains are referred to hereafter as M-D-11 and M-D-26 and the wet-aged grains as M-W-11 and M-W-26. Fig. 3 shows the ^{1}H CRAMPS and SP/MAS spectra of untreated and aged barley grains. The spectra in the left column of Fig. 3 were taken immediately following the aging treatment, and the spectra in the right column were taken after all grains were equilibrated to 33% RH. The CRAMPS spectra on the left-hand sides of Fig. 3 (*a*)–(*c*) reveal that the M-D-26 grain has lost intensity in the 4–7-ppm region relative to the spectrum of the untreated grain. The CRAMPS spectrum of M-W-26 shows an increase in overall linewidth, relative to that of the untreated grain. After the grains have been equilibrated to the 33% RH of the controlled storage environment, the overall CRAMPS spectra of aged and untreated grains are very similar, as seen by comparing the spectra on the right-hand sides of Fig. 3 (*a*)–(*c*). Apparently the spectral differences observed immediately following aging treatment reflect the humidity level of the treatment chamber. Equilibration of all of the grains to the same humidity level removes most of those spectral differences.

The SP/MAS spectra of aged and untreated grains shown in Fig. 3 (*d*)–(*f*) reveal the same trend as seen in the CRAMPS spectra ((Fig. 3 (*a*)–(*c*)). Immediately following aging, the M-D-26 grain produces a SP/MAS spectrum shown on the left side of Fig. 3 (*e*) that is lacking a significant water signal; the SP/MAS spectrum of the M-W-26 grain shown on the left side of Fig. 3 (*f*) contains a large water peak. The SP/MAS spectra shown on the right side of Fig. 3 (*d*)–(*f*) are of untreated and aged grains that were equilibrated to 33% RH before the NMR data were acquired and are very similar to each other. Thus, as with the CRAMPS spectra shown in Fig. 3 (*a*)–(*c*), the SP/MAS spectra shown in Fig. 3 (*d*)–(*f*), taken immediately following aging treatment, reveal some differences between the aged and untreated grains; but after equilibration to 33% RH, the spectra of untreated and aged (M-D-26, M-W-26) grains are much more similar to each other than the spectra taken before equilibration. Hence, no dramatic changes are observed in the ^{1}H CRAMPS and SP/MAS spectra as a result of the aging treatments.

CRAMPS and SP/MAS spectra of imbibed grains

Imbibition of fresh and aged barley grains was monitored by means of ^{1}H CRAMPS and SP/MAS. The CRAMPS and

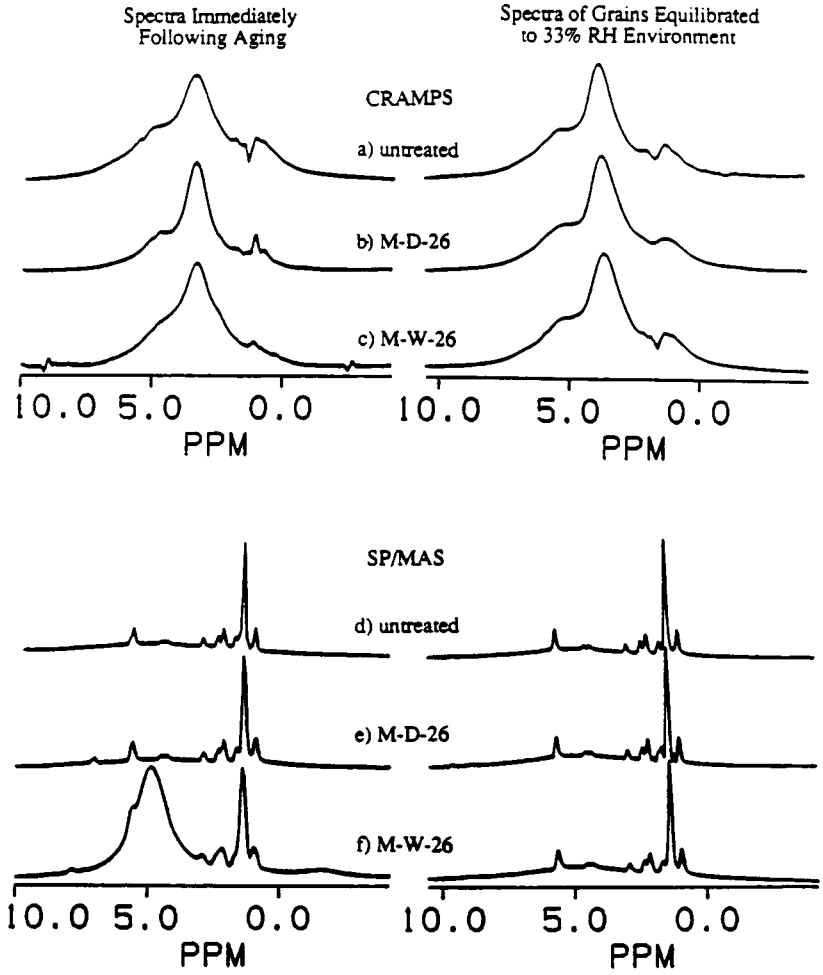

FIGURE 3 (*a*)–(*c*) ^{1}H CRAMPS and (*d*)–(*f*)SP/MAS spectra of untreated and artificially aged Moravian III barley grains. The spectra on the left were taken at 360 MHz immediately following the aging treatment, and the spectra on the right were taken at 187 MHz after the aged grains had reequilibrated to the controlled storage environment. CRAMPS spectra (*a*)–(*c*) were acquired by use of the BR-24 MP sequence.

SP/MAS results for fresh barley grains are given in Fig. 4, which shows results ranging from a grain in the unimbibed state containing 8.6% water, shown at the bottom of the figure, to a grain that has just germinated, with a water content of 34%, shown at the top of the figure. To yield these data, individual grains were imbibed to particular hydration levels; then each grain was weighed and used for the NMR experiments. (The same grain was not used in all experiments to avoid any effects from repeatedly starting and stopping imbibition. Some experiments were repeated several times to establish reproducibility among grains.) As the grain imbibes water, a peak at 4.7 ppm appears in the CRAMPS spectrum, and this new peak is assigned to water. As imbibition proceeds, the water peak grows in intensity and eventually dominates the spectrum.

The broad peak centered at ~4.7 ppm in the SP/MAS spectrum, which has been assigned to water of hydration in the unimbibed grain, grows in intensity as imbibition proceeds, and the linewidth of this peak decreases as imbibition progresses. This line narrowing reflects the increasing mobility of the water molecules as hydration sites on macromolecules are filled, as loosely bound water of hydration appears, and, finally, as "free" or capillary water appears in the grain.

"Free" and "bound" water have not been precisely defined in a universal context (Kuntz and Kauzmann, 1974). However, there is a consensus that "bound" water is restricted in motion and associated to some extent with hydration sites on macromolecules or ionic complexes, whereas "free" water has properties associated with pure liquid-state water. In this context, "free" water identified by NMR data in this paper and by previous workers (Seewaldt et al., 1981; Aksenov et al., 1982) behaves more as a liquid than the less mobile water identified as "bound" water.

An interesting absence from the ^{1}H SP/MAS spectra of imbibed barley grains in Fig. 4 is that of peaks caused by dissolved sugars. Chen et al. (1979) have observed dissolved sugars appearing in the ^{13}C NMR spectra of wild oat grains 2 days after germination. Colnago and Seidl (1983) have also observed the appearance of dissolved sugars in the ^{13}C NMR spectra of imbibed soybean seeds as early as 2.5 h after the start of imbibition. At least in the earlier stages of imbibition, before the water peak becomes dominant, one expects to observe the sugar resonances in the ^{1}H SP/MAS NMR spectra of the barley grain. The sugar -OH protons may exchange rapidly with water protons, preventing their separate observation; however, resonances resulting from the much less labile CH protons were expected, and their absence from the spectra is somewhat puzzling.

CRAMPS and SP/MAS results obtained on barley grains aged at 0% RH for 26 days (M-D-26) and obtained on grains aged at 100% RH for 26 days (M-W-26), quiescent and imbibed in water, are shown in Fig. 5. The imbibition of the M-D-26 grain proceeds qualitatively like that of the untreated grain, as observed by a comparison of the spectra in Figs. 4 and 5. The M-D-26 grains appear to be as vigorous as the untreated grains, as measured by the results of a 4-day germination assay, shown in Table 1. It is possible that very slight damage may have occurred in the M-D-26 grains during aging; if so, it has been mostly compensated for by repair mechanisms within the grain, the end result being vigorous seedlings. By comparing the spectra of Figs. 4 and 5, we see that the imbibition of the M-W-26 grain appears qualitatively very similar to that of fresh barley and M-D-26 barley. The one striking difference that is seen between spectra of imbibed M-W-26 barley grains and other imbibed grains is the increase in linewidth of the 4.7-ppm resonance observed in SP/MAS spectra of

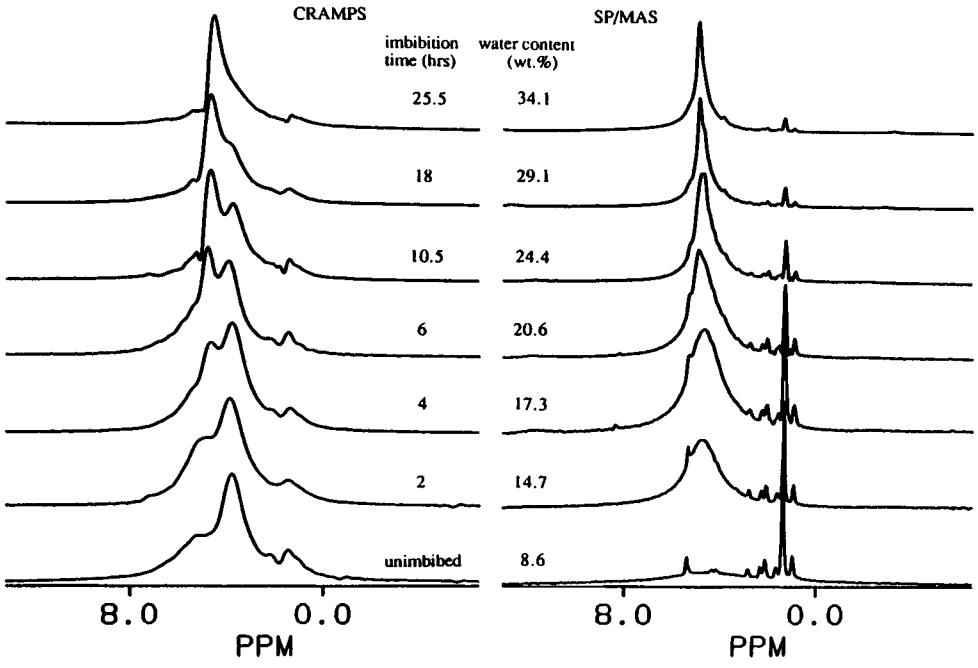

FIGURE 4 ^{1}H CRAMPS and SP/MAS spectra of imbibed, untreated Moravian III barley. Number of accumulations (*na*), 48–60; recycle delay (*rd*), 3.5 s.

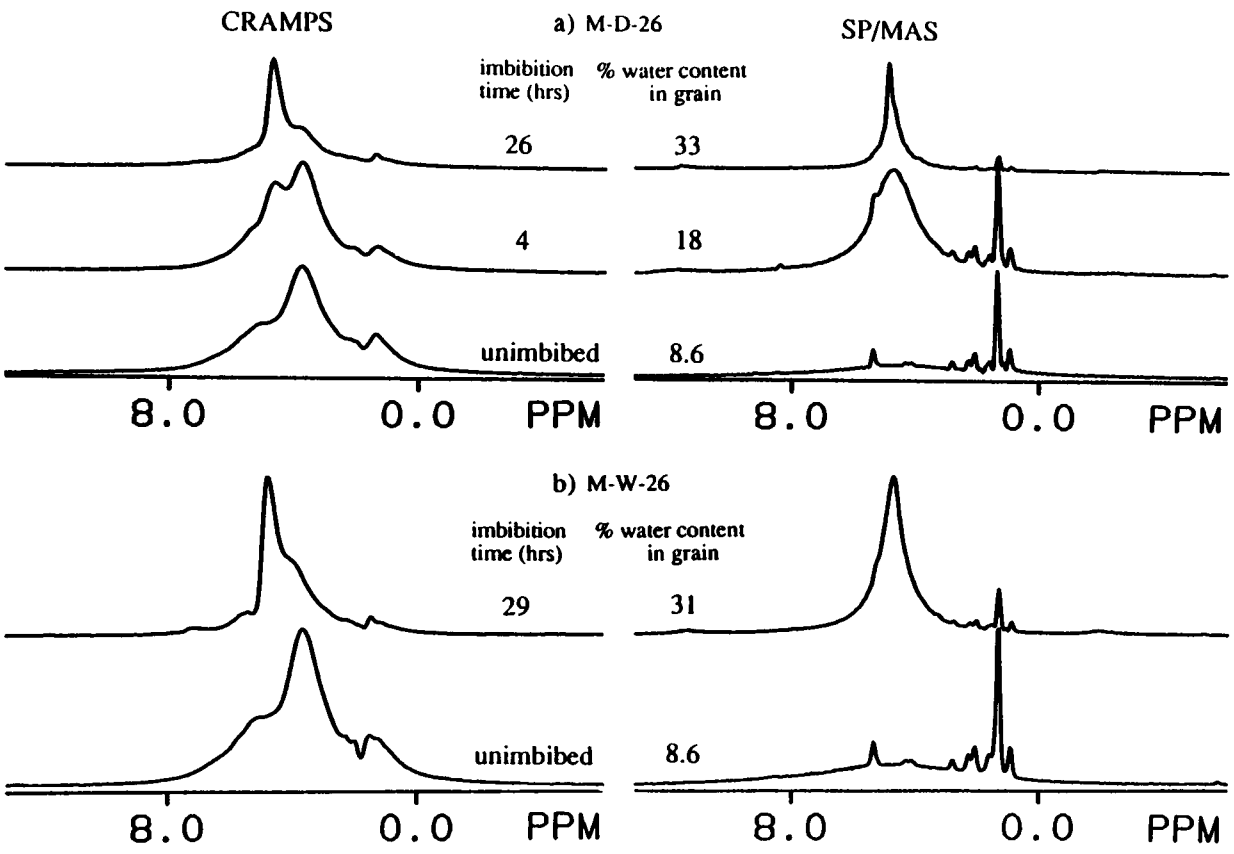

FIGURE 5 ^{1}H CRAMPS and SP/MAS spectra of imbibed, aged barley grains.

M-W-26 grains compared with the resonance in other imbibed grains. However, the M-W-26 grain is not viable; no M-W-26 barley grains have been observed to germinate during a germination assay, as seen in Table 1. Although the CRAMPS and SP/MAS spectra of the M-W-26 and other grains appear qualitatively similar to one another, differences between M-W-26 and other barley grains can be seen via relaxation experiments (vide infra).

An advantage of acquiring both ^{1}H CRAMPS and SP/MAS data for analysis of these barley samples is that each experiment highlights different components of the grain. The SP/MAS experiment provides good resolution of lipid and mobile water proton resonances without significant interference from starch and protein. The CRAMPS spectra provide some resolution of the two starch peaks; the protein and lipid resonances, although poorly resolved from the starch, also contribute significantly to the CRAMPS spectrum.

CRAMPS and SP/MAS spectra of excised embryos

Many models of seed aging propose that major factors in aging are lipid deterioration by peroxidative saturation of lipid double bonds and hydrolysis of triglycerides and phospholipids to form free fatty acids (Priestley, 1986; Harrington, 1973). Inasmuch as the embryo is the site of growth in a seed, it is generally thought that damage to embryonic tissue is more deadly to the seed than is damage to other seed tissues. With this in mind, ^{1}H CRAMPS and SP/MAS spectra were obtained on barley grain embryos excised from viable, untreated grains and from nonviable, wet-aged grains (M-W-11 and M-W-26). These spectra are shown in Fig. 6. The CRAMPS spectra of the embryos, shown in Fig. 6 (*a*), reveal lipid resonances and a broad feature attributed to rigid solids and bound water (referred to as "bound" because this feature is attenuated by dipolar dephasing for less than 1.5 ms (vide infra)). As the embryos of barley seeds contain much higher fractions of lipid than do the endosperm and the hull (Price and Parsons, 1979), the relative intensities of lipid peaks in Fig. 6 (*a*) are much higher than those in Fig. 3 (*a*)–(*e*). The SP/MAS spectra of the embryos are more useful for analyzing the lipids contained in the embryos because of the richness of the spectra; this can be seen by comparing the spectra of Fig. 6 (*a*) and (*b*).

The integrated intensities obtained from the peaks in the SP/MAS spectra of Fig. 6 (*b*) can be summarized as follows: 0.9 ppm, 3.0 (arbitrary scale); 1.3 ppm, 12.9 ± 0.8; 1.7 ppm, 2.5 ± 0.3; 2.0–2.3 ppm, 4.4 ± 0.3; 2.8 ppm, 1.2; 4.1–4.3 ppm. 1.1 ± 0.1; 5.3 ppm, 2.5 ± 0.3. The ratio of intensities of the 5.3- and 1.3-ppm peaks is 0.20 for each of the three samples. The methyl peak at 0.9 ppm is normalized to a value of 3.0 (for three methyl protons per fatty acid chain). The ratio of the intensities of the 5.3-ppm (vinyl proton) peak to the 1.3-ppm (bulk chain methylene protons) peak

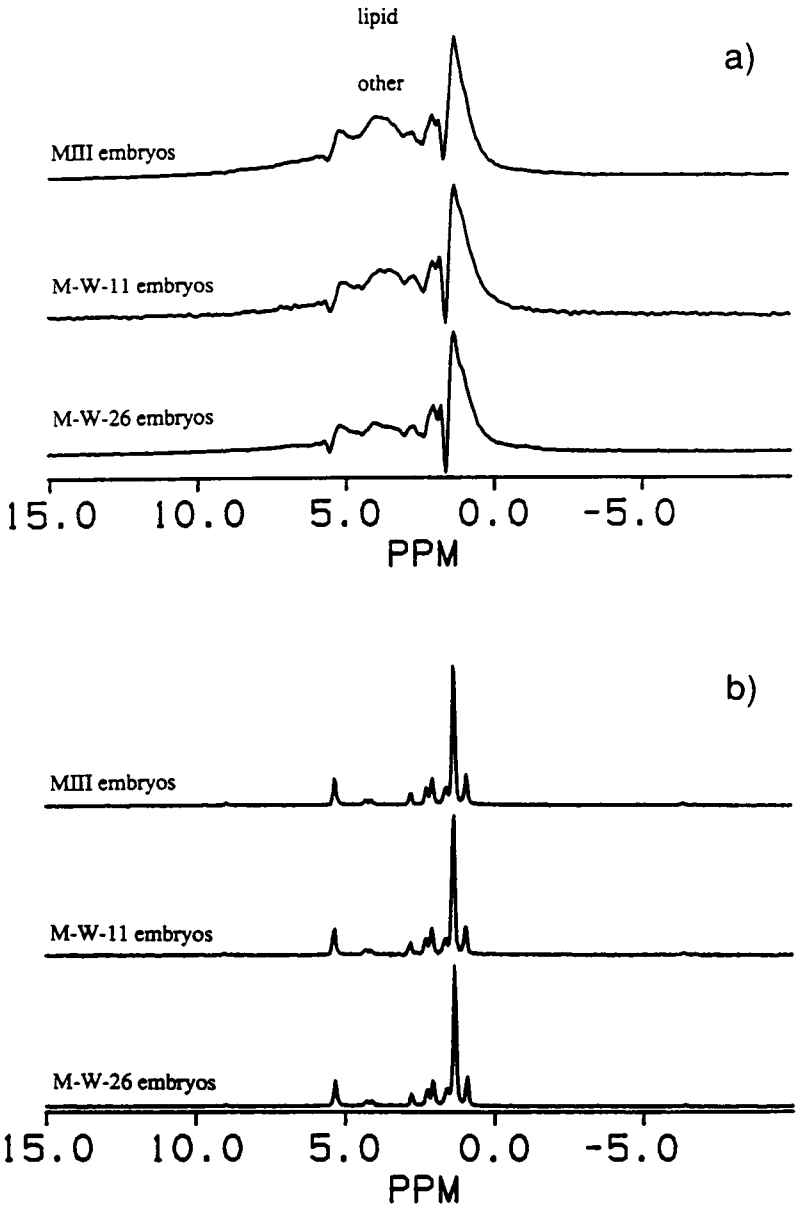

FIGURE 6 ^{1}H NMR spectra of excised barley-grain embryos taken from untreated (MIII) and wet-aged (M-W-11 and M-W-26) grains. (*a*) CRAMPS, (*b*) SP/MAS.

remains constant, within the limits of error, for the three embryo samples. If saturation of the lipid double bonds were occurring to a significant extent during aging, the M-W-11 and M-W-26 embryos ought to manifest relatively smaller spectral contributions from protons at 5.3 ppm than do the untreated, excised embryos; i.e., the 5.3-to-1.3-ppm intensity ratio should be smaller for aged embryos than for untreated embryos. A significant difference in that ratio is not observed in these data. If hydrolysis of triglycerides and/or phospholipids occurs in the embryos during aging of the grains, an increase in the intensities of the 4.1- and 4.3-ppm glyceride proton peaks ought to be observed in the spectra of the nonviable embryos, relative to the viable embryos. The relative intensities of these peaks do not increase, at least not more than approximately 5–10% (the estimated error limits).

If hydrolysis and double-bond saturation both occur as the barley grains age, then the intensity of the 5.3-ppm peak might not change in the spectra of the excised embryos. The 5.3-ppm peak contains contributions from glyceride and vinyl protons, and, although lipid hydrolysis can produce extra glyceride protons, double-bond saturation results in fewer vinyl protons. The glyceride proton peaks at 4.1 and 4.3 ppm do not increase in integrated intensity with aging. The lipid proton peak at 2.8 ppm represents proton on methylene carbons sandwiched between double bonds of polyunsaturated lipids; the intensity of this peak apparently remains constant with aging.

It is the polyunsaturated lipids that contribute intensity to the 2.8-ppm peak that are most susceptible to peroxidative attack in seeds (Harrington, 1973); thus, one would expect this peak to decrease in relative intensity with aging if the

degree of fatty acid unsaturation were increasing with aging. However, minor amounts of structural alterations that produce less than a 5% change in total intensity of a given peak would not be detectable in these spectra. If lipid degradation occurs during aging of these embryos by means of peroxidative saturation of the double bonds or by hydrolysis of triglycerides or phospholipids, it occurs to a degree that is not observable in these spectra.

^{1}H Relaxation in barley grains

The ability to resolve and identify particular molecular species within a spectrum allows one to assign relaxation behavior to the resolved components. Therefore, ^{1}H NMR relaxation rates can be measured for various species within the grain. One can minimize contributions from starch and protein species by appropriately choosing SP/MAS detection to monitor lipid and water relaxation rates. Relaxation measurements with CRAMPS detection can be used to gather information about starch and protein as well as about lipids and water.

^{1}H T_1 measurements

The T_1 (spin-lattice relaxation time) experiment monitors motion in a frequency regime at the laboratory-frame Larmor frequency (187 MHz in these experiments). A stack plot of ^{1}H CRAMPS T_1 relaxation spectra obtained on an untreated quiescent barley grain is shown in Fig. 7. The magnetization components giving rise to all the peaks are seen to relax at approximately the same rate. The total integrated intensity of each of the spectra in Fig. 7 was found to fit a single exponential curve of the form

$$M(t) = M(0)\exp(-t/T_1), \quad (1)$$

where $M(t)$ is the total intensity at time t and $M(0)$ is the intensity measured in an experiment in which the relaxation period is zero. CRAMPS proton spin-lattice relaxation rates were measured for each barley-grain sample represented in Figs. 4 and 5. The intensity data were fitted to Eq. 1, and the resulting T_1 values are presented in Table 2.

In homogeneous organic solids, one universal proton T_1 value for each substance is common, because of dipolar-mediated spin–spin flip-flops that give rise to efficient spin diffusion (Bloembergen et al., 1948). Although a seed is not a homogeneous solid, the protons observed in the CRAMPS T_1 experiment displayed in Fig. 7 show very similar relaxation behavior. ^{1}H spin-exchange experiments (Ridenour and Maciel, 1995) have shown that bound water protons can efficiently exchange polarization with both starch and protein protons on a time scale of ~100 ms. To a large extent, this spin-exchange process averages out T_1 differences among starch, protein, and water protons. Proton spin-lattice relaxation within the barley grain probably proceeds over a range of rates centered around the average rate observed. For example, starch deposited in starch grains of

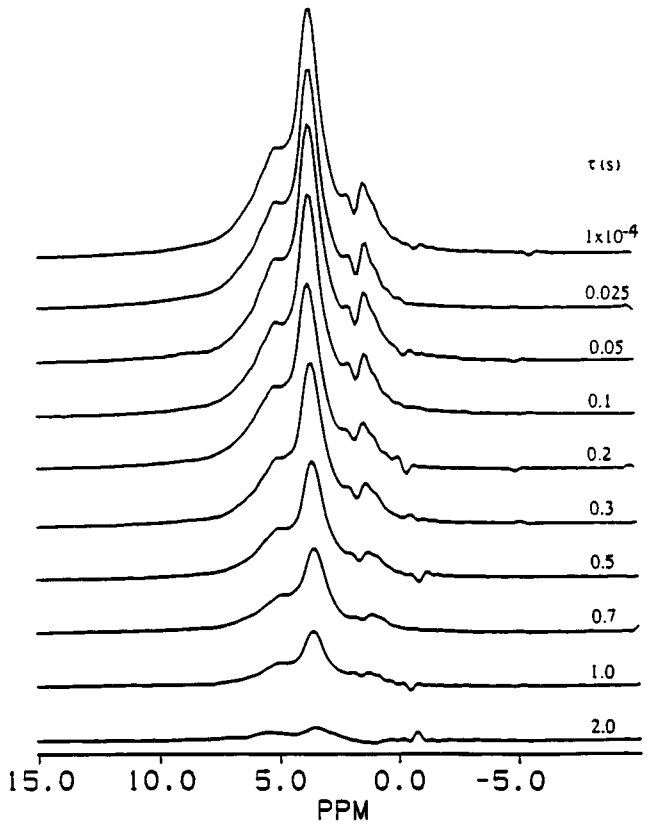

FIGURE 7 ^{1}H T_1 relaxation spectra of a quiescent Moravian III barley grain, monitored by the CRAMPS-detected Freeman–Hill technique. The BR-24 MP sequence was used, with *na* = 120 and *rd* = 5 s.

the endosperm and β-glucans present in aleurone layer cell walls both contain protons contributing to the peak at 3.7 ppm. These two carbohydrates may manifest different ^{1}H T_1 values, but the different decay rates, added together with other similar ^{1}H T_1 values for other protons in the barley grain, may appear to yield *approximately* a single, average result in the T_1 experiment. The relaxation may appear to fit a curve corresponding to a single exponential constant rather than a decay with a discrete number of exponential constants because of the large number of similar, but slightly different, T_1 contributions. However, substantial components (say, >10%) in such a distribution must not have T_1 values that differ widely from the measured "average" (by more than a factor of 2); otherwise a distinct relaxation component would be detected.

In analogy to spin-lattice relaxation measurements made with CRAMPS detection, proton T_1 values for the grains were also measured with detection under MAS only. A stack plot of spin-lattice relaxation spectra obtained with MAS-only detection for the quiescent, untreated barley grain is shown in Fig. 8. Because the MAS-only T_1 experiment detects primarily the most mobile seed components (weakest, motionally averaged dipolar interactions), separate T_1 behavior is detected for different peaks in the spectrum. The relaxation rates for lipid peaks at 0.8, 1.3, and 2.0 ppm (methylene, and allyl protons) and for the water peak

TABLE 2 ^{1}H T_1 values of Moravian III barley grain measured with CRAMPS or SP/MAS detection*

Imbibition		T_1 (s)‡				
			SP/MAS			
				Lipid (ppm)		
Imbibition Time (h)	% Water in Seed§	CRAMPS¶	Water (4.7 ppm)	2.0	1.3	0.8
Untreated						
0	8.6	0.67	0.72	0.41	0.39	0.68
0	8.6	0.66	0.58	0.37	0.37	0.60
0.5	12	0.42	0.35	0.35	0.38	0.50
1	12	0.44	0.41	0.35	0.40	0.67
2	15	0.34	0.29	0.37	0.35	0.50
4	17	0.31	0.25	0.33	0.40	0.55
6	21	0.27	0.25	0.32	0.38	0.55
10.5	24	0.25	0.22	0.19	0.37	0.56
18	29	0.17	0.21	0.32	0.34	0.48
25.5	34	0.15				
18/D_2O	28	0.45	0.50	0.39	0.41	0.63
M-D-26						
0	8.6	0.53	0.60	0.46	0.44	0.78
0	8.6	0.57	0.61	0.42	0.42	0.70
4	18	0.35	0.35	0.39	0.43	0.74
26	33		0.21	0.33	0.39	0.64
M-W-26						
0	8.6	0.62	1.1	0.42	0.37	0.67
29	31	0.28	0.25	0.29	0.34	0.46

*Freeman–Hill (1971) type technique used.
‡Estimated precision ± 10%.
§Fresh weight basis.
¶Based on total ^1H CRAMPS integral over the entire spectrum.

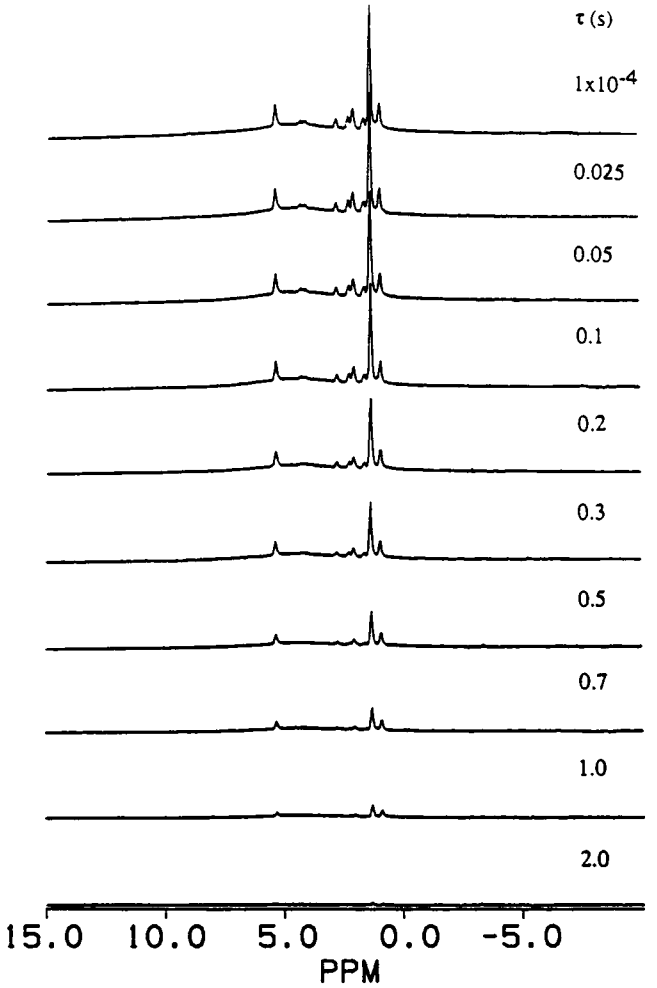

FIGURE 8 ^{1}H T_1 relaxation spectra of a quiescent Moravian III barley grain, monitored the Freeman–Hill technique with MAS-only detection. *na* = 120; *rd* = 5 s.

at 4.7 ppm were calculated by fits of individual plots of peak intensity versus time, using Eq. 1. Results of proton T_1 measurements obtained by MAS-only detection are also presented in Table 2.

Fig. 9 shows plots of the measured ^{1}H T_1 values versus the water content of the grains following imbibition. The CRAMPS T_1 data plotted in Fig. 9(*a*) show monotonic behavior that suggests a linear fit for % H_2O > 15% for the untreated barley grains (MIII, ▲). The first portion of the plot for the untreated grains (between the unimbibed state containing 8.6% water and the grain containing 15% water) is steep, with a negative slope. The proton T_1 value appears to change from ~0.7 to ~0.3 at the end of this early stage of imbibition. The decline in the value of T_1 at %H_2O ≃ 15% indicates that the proton-containing structures are being mobilized during early stages of imbibition, including the water protons that enter the grain. After the initial sharp decline, the proton T_1 continues to decrease, but more slowly, with increasing imbibition time (and increasing %H_2O). The point of germination is represented by the last data point, for the grain containing 34% water following imbibition.

The fit of proton T_1 values for the water peak obtained on untreated, imbibed barley grains by MAS-only detection is shown in Fig. 9 (*b*) as the solid curve, where it is seen to follow the pattern displayed for the total T_1 observed in the CRAMPS experiments for the same grains shown in Fig. 9 (*a*). In contrast, T_1 values observed by MAS-only detection for lipid protons in the barley grains (methyl *, methylene ×, and allyl ■ in Fig. 9 (*b*)) do not follow the biphasic pattern of sharp proton T_1 decline up to %H_2O ~ 15%, followed by modest proton T_1 decline during subsequent imbibition. The three dashed curves in Fig. 9 (*b*) are linear fits of proton T_1 data of untreated barley grains for the lipid proton methyl, methylene, and allyl peaks. Very slight variation in proton T_1 values is observed for the lipid protons in the barley grain as imbibition proceeds.

A comparison of proton T_1 values of M-D-26 and M-W-26 barley grains with proton T_1 values of the untreated grains does not reveal any striking differences. Considering grains in the quiescent state, the proton T_1 value measured by CRAMPS detection is lower for the aged than for the untreated grains. This may reflect proton mobilization in the aged grains that is due to partial fragmentation of some macromolecules during aging. However, the CRAMPS-detected proton T_1 value of the M-D-26 grain differs from that of the untreated grain more than the M-W-26 proton T_1

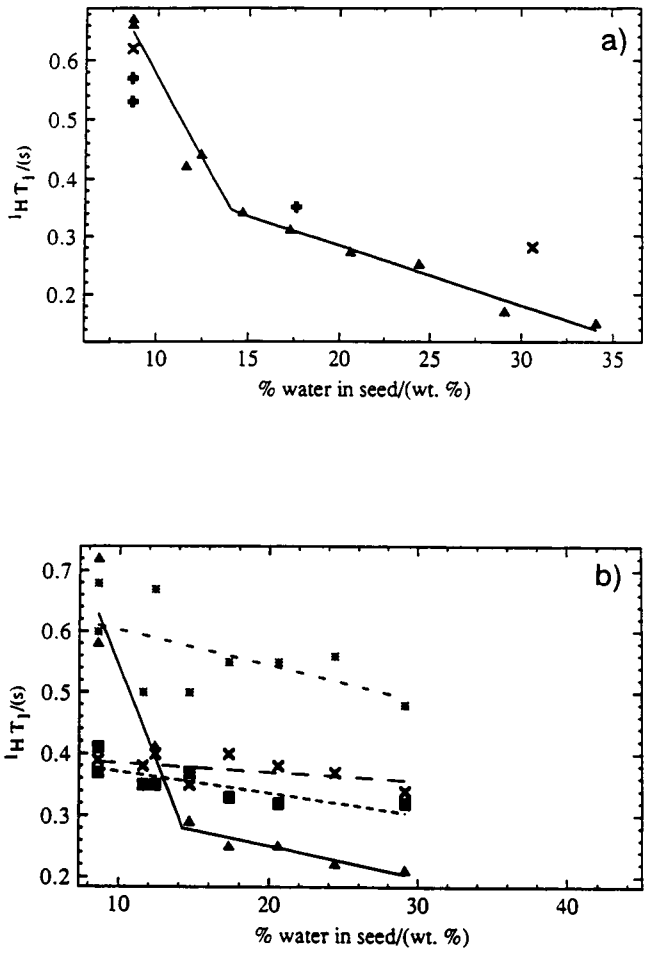

FIGURE 9 Plots of the ^{1}H T_1 values of barley grains versus imbibition period (represented in terms of increasing % water), *f*. The individual data points are taken from Table 2. (*a*) T_1 values measured for the total integrated spectrum by CRAMPS; the curve is a fit of the T_1 data for untreated MIII barley grains; data points: ▲, MIII; +, M-D-26; ×, M-W-26. (*b*) T_1 values for MAS-only detected spectra; the solid curve is a fit of the water peak data for untreated barley; the dashed curves are fits of the T_1 data for lipid peaks in untreated barley (- - - -, methyl peak; ——, allyl peak; – – –, methylene peak); data points: *, methyl peak; ▲, water peak; ■, allyl peak; ×, methylene peak.

value differs from that of the untreated grain. Yet, it is the M-W-26 grain, and not the M-D-26 grain, that has lost all viability. Thus, if the difference in proton T_1 values between the quiescent grains were an indicator of aging, one would have expected a larger difference for the M-W-26 grain relative to the untreated grain in comparison with the M-D-26 grain relative to the untreated grain.

A comparison of imbibed grains shows that the proton T_1 value measured by CRAMPS for the imbibed M-W-26 grain is significantly displaced from the linear T_1 fit for the untreated grains. The M-W-26 grain was imbibed to a water level of 31%, and a CRAMPS-detected T_1 value of 0.28 s was measured for that grain. The proton T_1 value for an untreated grain imbibed to a water level of 31% would be 0.17 s, according to the T_1 fit shown in Fig. 9 (*a*) for the untreated grains. Based on this fit of the T_1 data for the untreated grains, the CRAMPS-detected T_1 value of 0.28 s measured for the imbibed M-W-26 grain corresponds to the CRAMPS-detected proton T_1 value for an untreated grain imbibed to only 21% water. Thus, the CRAMPS-detected proton T_1 value measured for the imbibed M-W-26 grain corresponds to a CRAMPS-detected proton T_1 value for an untreated grain that has imbibed less water. Because the observed decrease of the proton T_1 value during imbibition is interpreted as resulting from proton mobilization, it is speculated that these T_1 data for the imbibed M-W-26 grain indicate that less mobilization of proton-containing structures occurs during imbibition of the M-W-26 grain relative to the untreated grain.

^1H T_2 measurements

Proton T_2 values were measured on the various barley grains by CRAMPS detection as well as by detection under MAS only. T_2 values measure the rate of dephasing of nuclear spin magnetization in the transverse (*xy*) plane (relative to the static magnetic field along *z*). For solids, T_2 values are typically determined by static interactions, e.g., dipolar couplings. For example, the transverse proton magnetization in a rigid —$(CH_2)_n$— chain dephases rapidly, with a time constant as small as 10^{-6}-10^{-5} s. If, however, the —$(CH_2)_n$— chain is in rapid motion, as in a lipid membrane chain, the dipolar couplings between protons are not so strong, and the ^{1}H magnetization dephases more slowly, corresponding to larger proton T_2 values. Thus, T_2 becomes larger as the proton-containing structures are mobilized.

CRAMPS and SP/MAS spectra obtained with different dephasing times on a quiescent, untreated barley grain are shown in Figs. 10 and 11, respectively. The ^{1}H magnetization giving rise to starch and protein peaks shown in Fig. 10 dephases rapidly, as is characteristic of rigid molecules, and is fully dephased in the CRAMPS spectra of Fig. 10 obtained with dephasing periods greater than 0.68 ms. The water peak, which is the broad feature centered at 4.7 ppm in the SP/MAS spectrum of Fig. 11, is completely dephased by 0.68 ms. Only the slowly dephasing components that are due to lipid resonances remain in the CRAMPS and SP/MAS spectra of Figs. 10 and 11 that correspond to long dephasing periods.

^{1}H dipolar dephasing was performed on quiescent and imbibed grains for both untreated and aged grains, with both CRAMPS and MAS-only detection. The dephasing time constants, T_2, were calculated by fitting the data to the following equation:

$$M(t) = M_G(0)\exp(-t^2/2T_{2G}^2) + \sum_i M_{Li}(0)\exp(-t/T_{2Li}), \quad (2)$$

where $M(t)$ and $M(0)$ are the intensities at dephasing times t and zero, respectively. Equation 2 contains a Gaussian term, with a time constant, T_{2G}, that fits only those CRAMPS data containing the fastest dephasing compo-

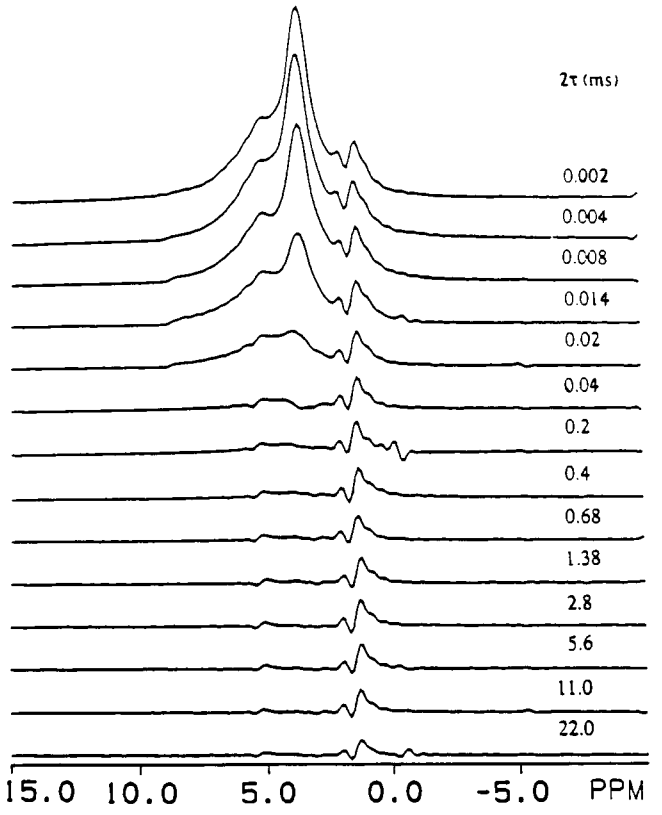

FIGURE 10 ^{1}H T_2 relaxation spectra of a quiescent Moravian III barley grain, monitored by the CRAMPS-detected Hahn spin-echo technique, with *na* = 120 and *rd* = 5 s. The period 2τ represents the time period between the first radio-frequency pulse and the start of data acquisition.

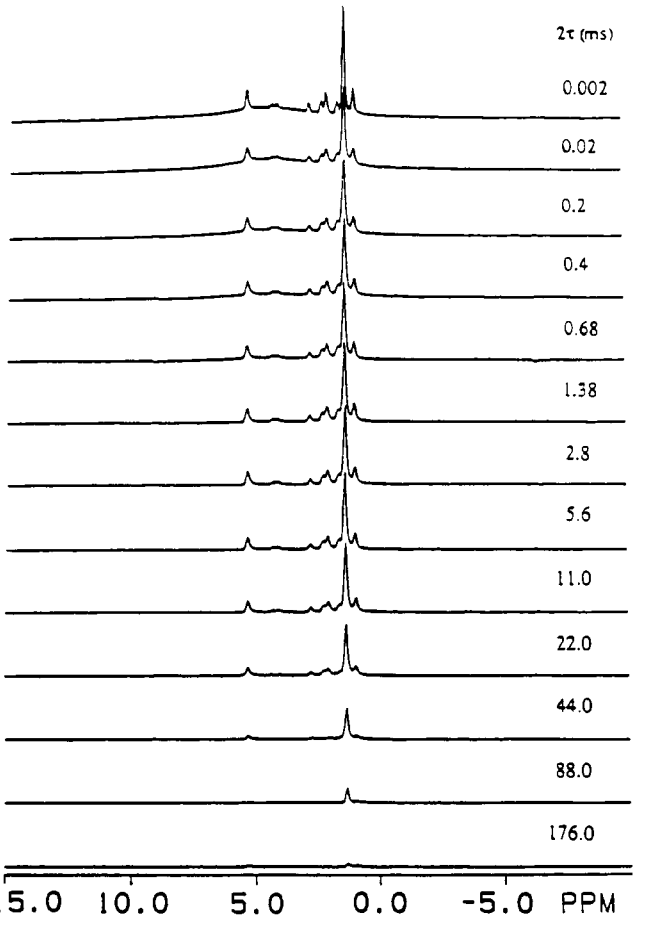

FIGURE 11 ^{1}H T_2 relaxation spectra of a quiescent Moravian III barley grain, monitored by the T_2 Hahn echo experiment with MAS-only detection, with *na* = 120 and *rd* = 5 s. The period 2τ represents the time period between the first radio-frequency pulse and the start of data acquisition.

nents. The Lorentzian terms, with time constants T_{2L}, describe the dephasing behavior of all the slowly dephasing components. The MAS-only detected dephasing data can all be fitted with $M_G(0) = 0$ in Eq. 2, i.e., with only slowly dephasing Lorentzian terms.

To assign dephasing components to spectral features, we separated the CRAMPS spectra into specific regions of intensity for data analysis; deconvolutions of these spectra were not used because of problems with reproducibility and reliability in deconvolution in spectra of this type. The three regions chosen for the CRAMPS data analysis center around the peaks at 1.3, 3.7, and 4.9 ppm. The spectral regions used for the integration are 0.5 to 1.6, 2.6 to 4.1, and 4.1 to 7.0 ppm. The MAS-only detected spectra contain sufficient resolution that peak heights can be used for individual peaks, and dephasing was monitored for peaks centered at 0.8, 1.3, 2.0, 4.7, and 5.3 ppm. Even though it is highly probable that a wide range of dephasing time constants is represented in the grains, especially as imbibition proceeds, in most cases the dephasing data did not warrant more than a one- or two-component fit for each peak (MAS-only) or spectral region (CRAMPS). Only where the data for a particular integral region justified a distinctly three-component fit was such an analysis employed. The calculated T_2 values for the dephasing data detected by CRAMPS and MAS-only are summarized in Tables 3 and 4, respectively.

The measured T_2 values obtained by CRAMPS for the quiescent, untreated barley grain listed in Table 3 can be associated with three motional regimes. The fast Gaussian decay components with T_{2G} = 11–12 μs, measured for all three intensity regions, are each associated with a rigid lattice; the slow Lorentzian component of 28 ms, measured for the integrated region around 1.3 ppm, is characteristic of a highly mobile proton environment; the intermediate Lorentzian component of 1.1 ms, measured for the integrated region around 4.9 ppm, corresponds to protons in an intermediate motional regime in which dipolar couplings are partially averaged by motion (Jurkiewicz et al., 1989, 1990). The Gaussian decay component is assigned to rigid-lattice protons of macromolecules, including starch and protein. The intermediate Lorentzian component is assigned to water protons; the value of 1.1 ms corresponds reasonably well to bound waters of hydration (Aksenov et al., 1982). Lipid proton dephasing behavior is slow because of the rapid rotation of the lipid chains and is represented by the slow Lorentzian decay component. T_2 values measured

TABLE 3 ^1H T_2 values of Moravian III barley grain measured with CRAMPS detection*

Imbibition		T_2 (ms)‡					
Imbibition Time (h)	% Water in Seed§	Water and Carbohydrate (4.9 ppm)		Carbohydrate (3.7 ppm)		Lipid and Protein (1.3 ppm)	
Untreated (MIII)							
0	8.6	0.012¶	(89%)	0.011¶		0.012¶	(67%)
		1.1	(11%)			28	(33%)
2	15	0.014¶	(70%)	0.012¶	(84%)	0.015¶	(65%)
		1.7	(30%)	1.7	(16%)	22	(35%)
4	17	0.017¶	(52%)	0.012¶	(82%)	0.015¶	(59%)
		2.3	(48%)	1.9	(18%)	22	(41%)
6	21	0.015¶	(42%)	0.013¶	(80%)	0.017¶	(60%)
		1.6	(58%)	2.0	(20%)	21	(40%)
10.5	24	0.026	(41%)	0.021	(76%)	0.028	(50%)
		3.1	(59%)	4.6	(24%)	26	(50%)
18	29	0.025	(37%)	0.014¶	(65%)	0.018	(69%)
		3.0	(63%)	2.5	(35%)	31	(31%)
25.5	34	0.018	(17%)	0.015	(57%)	0.022	(48%)
		0.87	(40%)	0.72	(21%)	0.73	(17%)
		7.4	(43%)	9.6	(22%)	26	(35%)
18/D_2O	28	0.026	(47%)	0.014¶		0.021	(55%)
		0.34	(13%)			26	(45%)
		3.9	(40%)				
M-D-26							
0	8.6	0.013¶	(88%)	0.011¶		0.012¶	(63%)
		0.41	(12%)			26	(37%)
4	18	0.014¶	(56%)	0.026		0.026	(52%)
		1.3	(44%)			27	(48%)
M-W-26							
0	8.6	0.014¶	(89%)	0.010¶	(97%)	0.0088¶	(68%)
		0.73	(11%)	1.7	(3%)	23	(32%)
29	31	0.046	(54%)	0.020	(83%)	0.025	(70%)
		3.2	(46%)	4.4	(17%)	27	(30%)

*Hahn spin-echo type technique used.
‡Estimated precision ± 20%.
§Fresh weight basis.
¶Gaussian fit to T_2 decay curve.

by MAS-only detection for the quiescent, untreated grain listed in Table 4 all correspond to intermediate and slow Lorentzian decays. A Gaussian component is not observed by dephasing with MAS-only detection because the protons that contribute to Gaussian decay are those protons in a rigid lattice with strong dipole–dipole interactions and are not substantially represented by SP/MAS techniques.

Proton dephasing (T_2) results are also presented in Tables 3 and 4 for imbibed barley grains. However, before these results are discussed, comments on the utility of these types of data are warranted. Imbibed grains exist in a state of change, and therefore experiments that rely on the dynamics of the system, such as proton dephasing measurements, reflect the time-averaged status of the system during the experiment. The proton spectra of imbibed grains (CRAMPS or SP/MAS) obtained without dephasing appear to be essentially the same, whether they are obtained immediately following imbibition or several hours following cessation of imbibition. However, if a dephasing interval is applied before detection, the spectra are not invariant under a period of elapsed time following imbibition. Fig. 12 shows, for a grain imbibed for 4 h to a water content of 18%, CRAMPS and SP/MAS spectra obtained with a dephasing interval of 0.72 ms inserted before detection. Each spectrum of Fig. 12 represents 10 min of data acquisition. The elapsed time between stopping imbibition and starting data acquisition for a particular spectrum is shown on the right of that spectrum. The total postimbibition time elapsed from the first to the last experiments is 3 h, 20 min. Hence, the changes that occurred within the grain after imbibition was stopped were monitored for more than 3 h.

Fig. 12 clearly shows that, as the time following imbibition increases, the water peak that remains in both the CRAMPS and SP/MAS spectra *after dephasing* decreases in intensity and increases in linewidth. Integration of the water peak that remains after dephasing reveals that there is a decrease in total integrated intensity of the peak, or a loss of proton signal, as the time after imbibition increases. If water were being lost from the grain after imbibition was stopped, the *undephased* (normal) CRAMPS and SP/MAS spectra would change; but they do not. This decrease in water-proton intensity following dephasing is an indication that water, after imbibition ceases, redistributes in the grain to more rigid sites, with a correspondingly smaller T_2. If the T_2 value becomes smaller for a given set of protons, then less signal intensity will survive a given dephasing period for CRAMPS or MAS-only detection following that dephasing period, e.g., in the spectra of Fig. 10, several hours after imbibition has stopped. As a smaller water-proton T_2 value corresponds to more tightly bound water, it appears that, as the postimbibition time increases, some water molecules are "redistributed" within the grain to regimes that are more rigid than the regimes that they occupied during imbibition. Note that "redistribution" here does not necessarily imply a *spatial* redistribution of water but may be characterized by a redistribution of *motional states*. The water molecules that are redistributed to more rigid sites during the time elapsed after imbibition most likely participate in hydration of macromolecules and probably also affect the proton dephasing behavior of those components of the grain.

The broadening of the water peak that is observed in the dipolar-dephased CRAMPS results in Fig. 12 is most likely a result of a broader dispersion of chemical shifts for the water protons, resulting from distribution of the water to a variety of chemically distinct sites. The broadening of the water peak observed in the dipolar-dephased MAS-only spectra of Fig. 10 could be the result of an increase in chemical shift dispersion and/or of a slight increase in rigidity and dipolar couplings of the water protons, leading to a slight decrease in T_2 and correspondingly to a broader NMR line.

From the results summarized in Fig. 12 it is clear that the proton dephasing behavior in imbibed grains is not independent of the time interval between the end of the imbibition period and the start of the NMR experiment. Keeping this in mind, one should realize that the dephasing experi-

TABLE 4 ^1H T_2 values of Moravian III barley with SP/MAS detection*

Imbibition			T_2 (ms)‡							
			Lipid Peaks (ppm)							
Imbibition Time (h)	% Water in Seed§	Water (4.7 ppm)	5.3		2.0		1.3	0.8		
Untreated										
0	8.6	0.37	0.30	(42%)	0.19	(29%)	47	0.18	(22%)	
			33	(58%)	23	(71%)		31	(78%)	
2	15	1.0	0.67	(66%)	0.22	(28%)	46	0.34	(27%)	
			25	(34%)	19	(72%)		37	(73%)	
4	17	0.25 (22%)	0.93	(69%)	0.25	(27%)	53	0.13	(34%)	
		2.2 (78%)	16	(31%)	20	(73%)		44	(66%)	
6	21	0.39 (30%)	0.74	(63%)	0.29	(27%)	44	0.27	(17%)	
		2.9 (70%)	12	(37%)	17	(73%)		23	(83%)	
10.5	24	0.94 (42%)	1.5	(71%)	0.24	(26%)	52	0.32	(18%)	
		5.6 (58%)	19	(29%)	20	(74%)		34	(82%)	
18	29	0.71 (33%)	1.7	(79%)	0.77	(15%)	48	0.20	(13%)	
		9.4 (67%)	24	(21%)	20	(85%)		23	(87%)	
25.5	34	1.0 (30%)	2.5	(84%)	0.71	(34%)	43	0.33	(27%)	
		11 (70%)	30	(16%)	20	(66%)		26	(73%)	
18/D_2O	28	0.31 (14%)	0.76	(36%)	19		42	0.30	(10%)	
		3.4 (86%)	19	(64%)				30	(90%)	
M-D-26										
0	8.6	0.32	0.22	(42%)	0.19	(28%)	46	0.22	(18%)	
			29	(58%)	23	(72%)		26	(82%)	
0	8.6	0.32	0.17	(32%)	0.19	(22%)	49	0.20	(16%)	
			33	(68%)	24	(78%)		31	(84%)	
4	18	0.31 (24%)	0.76	(67%)	1.5	(39%)	41	0.68	(11%)	
		1.5 (76%)	19	(33%)	24	(61%)		27	(88%)	
26	33	0.43 (23%)	2.1	(75%)	18		49	30		
		9.4 (77%)	18	(25%)						
M-W-26										
0	8.6	0.40	0.23	(42%)	0.17	(29%)	40	0.12	(23%)	
			25	(58%)	20	(71%)		27	(77%)	
29	31	1.5 (78%)	1.5	(87%)	2.2	(27%)	38	0.85	(26%)	
		5.2 (22%)	19	(13%)	19	(73%)		28	(74%)	
72	45	0.25 (20%)					39			
		12 (80%)								

*Hahn (1950) spin-echo method.
‡Estimated precision ± 20%.
§Fresh weight basis.

ments were all performed over a period of a period of 1–3 h, as the determination cannot be made instantaneously. Therefore, the T_2 values presented in Tables 3 and 4 are *averages* over that period and are more representative of grains several hours *following* an imbibition period than they are of the system *during* the dynamic process of germination. Changes in the system that occur during the NMR measurements are likely to produce effects on the measured T_2 value that are difficult to quantify. Nevertheless, the orders of magnitude of the reported T_2 values, the general trends in larger T_2 values with imbibition time, the trends in percent contribution resulting from the signals of individual T_2 decay components, and the distinction between Gaussian and Lorentzian decays are consistent and reproducible qualitative trends and are most probably significant.

As imbibition of the barley grain is initiated and proceeds to an increasing extent, the relative contribution of the Gaussian decay component to the overall CRAMPS-observed decay decreases and the contribution for Lorentzian components increases. Midway through germination, between the hydration levels of 24% and 29% water (see Table 3), the fast-dephasing component switches from a Gaussian decay to a fast Lorentzian decay. The Lorentzian component that dephases at an intermediate rate manifests a larger T_2 value and increases in its relative contribution to the 3.7- and 4.9-ppm peaks as imbibition proceeds from quiescence to 29% water content. When germination is complete, represented by the grain with 34% water, the CRAMPS dephasing results of Table 3 show three Lorentzian dephasing components for each peak, corresponding to fast, intermediate, and slow Lorentzian behavior.

Proton dephasing behavior was also monitored for the M-D-26 and M-W-26 grains through CRAMPS detection; the T_2 values are reported in Table 3. The proton dephasing behavior of the M-D-26 grain is virtually identical to that of the untreated grain. Proton dephasing of the M-W-26 grain differs from that of the untreated grain significantly only in

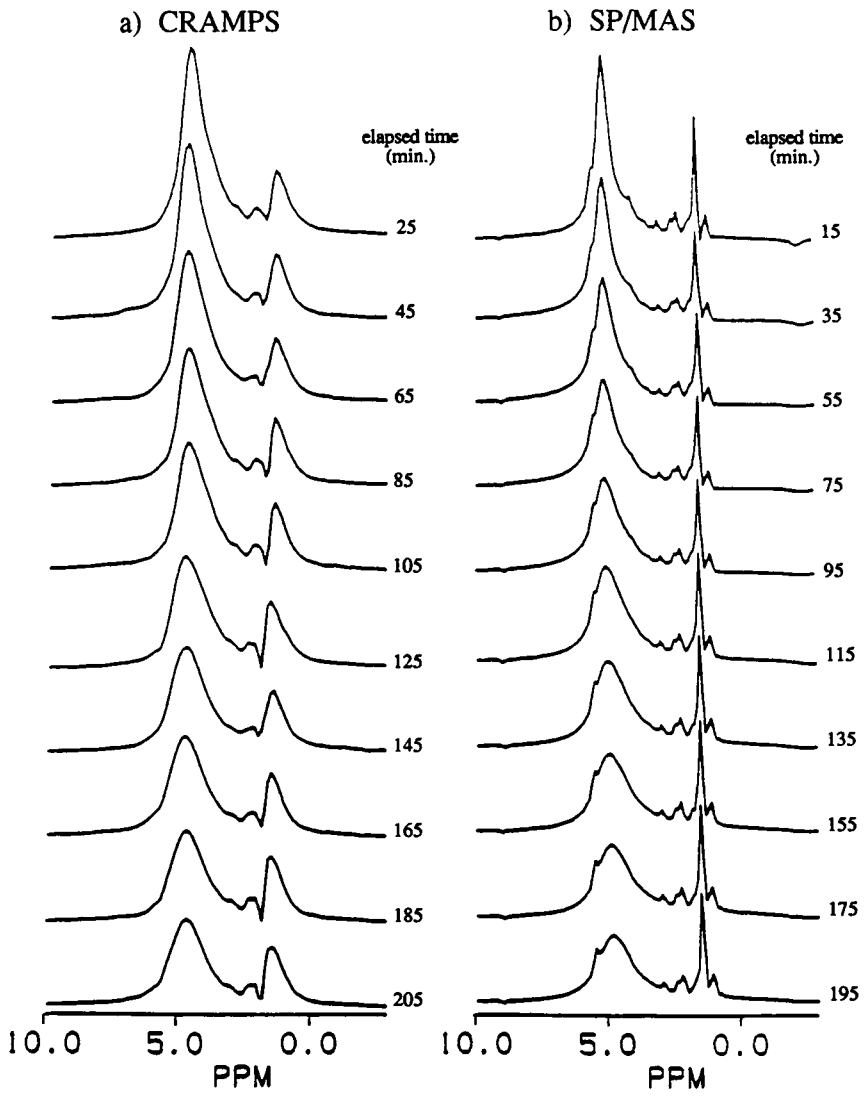

FIGURE 12 Time elapse (*a*) ^{1}H CRAMPS and (*b*) SP/MAS NMR spectra acquired on an untreated barley grain imbibed for 4 h with a water content of 18%. The top spectra were acquired first and the bottom spectra were acquired last. A 0.72-ms dephasing interval was employed following excitation and before detection of the spectra.

that the relative contribution of the fast Lorentzian component to the total intensity of the 3.7- and 4.9-ppm peaks is larger for the imbibed M-W-26 grain than for the untreated grains at comparable hydration levels.

The T_2 values obtained on imbibed grains with MAS-only detection, given in Table 4, monitor primarily the dynamics for the water and lipid protons. Lipid proton T_2 values do not vary markedly with imbibition. The methylene protons at 1.3 ppm manifest a T_2 value of 47 ms in the quiescent grain, corresponding to a highly mobile regime. The T_2 value for these protons remains the same throughout imbibition, within the limits of experimental error. The lipid protons at 5.3, 2.0, and 0.8 ppm exhibit biphasic dephasing behavior in the quiescent grain, with a slow Lorentzian component corresponding to highly mobile lipid regions and an intermediate Lorentzian component reflecting restricted motion. The 2.0- and 5.3-ppm lipid peaks, both associated with unsaturated lipid regions, have intermediate Lorentzian decay components that manifest larger T_2 values with increased imbibition time. The T_2 value of the intermediate Lorentzian component changes by a factor of ~10 from quiescence to germination for the 5.3-ppm peak and by a factor of ~2.5 for the 2.0-ppm peak. The proton dephasing data for only the 5.3-ppm peak reveal a change in the relative contributions of intermediate-Lorentzian and slow-Lorentzian components during imbibition. In part, this may be an experimental artifact resulting from the increasing domination and overlap of the 5.3-ppm lipid peak by the nearby water peak at 4.7 ppm as imbibition proceeds, making it difficult to obtain good intensity information on the 5.3-ppm peak for small dephasing times.

The water proton dephasing behavior, as observed by MAS-only detection, starts out in the quiescent grain as an intermediate Lorentzian decay and becomes biphasic at the stage of imbibition corresponding to a hydration level of 17%. The relative contributions of the two decay components do not change very much for grains with hydration levels between 17% and 34% (germination), although the slower decay becomes even slower as imbibition proceeds.

Dephasing constants measured for the water peak by MAS-only and CRAMPS do not agree perfectly.

Difficulties in measurement mentioned above may be partly responsible for the discrepancy. Also, the water peak observed by CRAMPS contains a substantial contribution from carbohydrate protons as well as from any immobile water that may be present. As mentioned above, the data usually do not warrant more than a two-component fit. Therefore, the CRAMPS T_2 data for barley grains up to a hydration level of 29% are fitted to one fast (Gaussian) component for the carbohydrate and one slow (Lorentzian) component to describe the water-proton dephasing behavior. The MAS-only water peak does not contain a contribution from rigid-lattice carbohydrate protons, and so the water decay curve can be more readily split into two components. In any case, the relaxation behaviors measured by CRAMPS and MAS-only detection are not expected to agree perfectly for complex systems such as a barley grain, because CRAMPS and SP/MAS spectra characteristically emphasize proton-containing species of different motional regimes.

T_2 results obtained with the M-D-26 and M-W-26 grains by MAS-only detection follow the same trends with imbibition as those discussed above for the untreated grains. The treated grains maintain slow Lorentzian decay components for the lipid proton peaks and intermediate decay components for all but the 1.3-ppm peak. As imbibition proceeds, the T_2 value of the intermediate-rate Lorentzian components of the 2.0- and 5.3-ppm peaks increases. The M-W-26 grain shows some striking differences in the pattern of water-proton dephasing behavior with imbibition relative to the behaviors of the M-D-26 and untreated grains. After the M-W-26 grain imbibes water to a content of 31%, the ratio of the contribution of the intermediate Lorentzian decay component to that of the slow Lorentzian decay component for the water peak is ~4:1. The untreated grains and the M-D-26 grains all show an intermediate-to-slow ratio between 1:1 and 1:4 once imbibition is under way. Only after a much longer imbibition period of 72 h (but still without germination) does the M-W-26 grain show an intermediate-to-slow ratio of Lorentzian decay rates that resembles that of the other grains.

The saturation of double bonds in membrane lipids is proposed to occur in seeds during aging, and membrane fluidity is known to decrease as the level of saturation increases (Harrington, 1973). To assess the mobility of the lipids contained within the barley-grain embryo as a function of aging, we measured T_2 values by MAS-only detection for viable (untreated, MIII) and nonviable (M-W-11 and M-W-26) embryos. T_2 values for the 0.9-, 1.3-, 2.0-, and 5.3-ppm peaks (methyl, methylene, allyl, and vinyl protons, respectively) were measured. These T_2 results are summarized in Table 5. The T_2 values measured for the 1.3-, 2.0-, and 5.3-ppm lipid proton peaks may decrease slightly with aging, but the decrease observed in these data is not significantly greater than the error limits. Although the T_2 value obtained for the methyl protons in MIII embryos is significantly larger than that in M-W-11 embryos, the value obtained for the methyl protons of the M-W-26 embryos is not significantly different from the value obtained from the untreated embryos. Thus, there is no clear trend between embryonic-lipid proton T_2 values and time of aging in these grains.

TABLE 5 ^{1}H T_2 values of viable (MIII) and nonviable (M-W-11 and M-W-26) embryos, excised from Moravian III barley, obtained with SP/MAS detection*

	T_2 (ms) Peak (ppm)‡			
Embryo	5.3	2.0	1.3	0.9
MIII	33	24	44	30
M-W-11	34	23	42	37
M-W-26	26	20	40	28

*Hahn (1950) spin-echo method.
‡Estimated precision ± 20%.

Imbibing grains in D_2O might seem attractive for eliminating interference from water protons in the proton NMR spectrum. Indeed, barley grains will germinate in 99% D_2O, and the proton spectrum reveals only a relatively small water peak even after long imbibition times. However, proton T_1 and T_2 data obtained for barley grains imbibed in D_2O are very different from data obtained for H_2O-imbibed grains. The difference in relaxation behavior is not surprising, because protons contained in the D_2O-imbibed grains are more isolated from other protons than in the H_2O-imbibed grains. Relaxation data on a representative barley grain imbibed in D_2O for 18 h to a water content of 28%, summarized in Tables 2–4, demonstrate the magnitude of the D_2O-vs.-H_2O difference. The ^{1}H CRAMPS T_1 value of the grain imbibed in D_2O for 18 h is comparable with the value measured for a grain imbibed in H_2O for only 1 h. However, the D_2O-imbibed grain contains more than twice as much water as the grain imbibed in H_2O for 1 h. Likewise, for MAS-only detection, the D_2O-imbibed grain has a proton T_1 value that is larger than the T_1 value measured for an untreated grain imbibed to the point of similar water content. Based on the ^{1}H T_1 values alone, one would place the D_2O-imbibed grain at a very early stage of imbibition.

The proton T_2 values of the D_2O-imbibed grain are not very different from the T_2 values of grains imbibed in H_2O for similar periods of time. Nevertheless, one should exercise great care in using relaxation measurements to monitor complex biological processes in a system that contains such a high level of deuterium. Even though barley grains will germinate in 99% D_2O, the resulting seedlings will not grow in 99% D_2O. Thus, metabolic and physical processes in the D_2O imbibed grain may be radically different from those in a normal grain. In any event, although the interference of water protons is removed from the proton NMR spectrum in D_2O-imbibed grains, relaxation data for the remaining protons are altered and are not a good indicator of normal processes. Hence, especially in view of their distinct ^{1}H T_1 dynamics, D_2O-imbibed grains were not investigated as models for advanced stages of imbibition.

Discussion of relaxation results

Overall, the proton relaxation data obtained on the barley grains provides information on the dynamics of the grain components during imbibition. The most efficient spin-lattice relaxation of a spin system occurs when motions present in the system have correlation times, $\tau_c \cong \omega_o^{-1} n$, where ω_o is the Larmor frequency (187 MHz here). In quiescent grains, the correlation times for motion in bound water and macromolecules are most likely too large for this optimum proton T_1 relaxation efficiency, because most of the grain components are rigid, solid macromolecules; the motions present are small in amplitude and have large correlation times.

As imbibition is initiated in barley grains, the CRAMPS-detected proton T_1 value and MAS-only detected T_1 value for water protons decrease in the grain. This behavior is most likely due to an increase of the τ_c^{-1} and amplitude of motions of the proton-containing structures in the barley grain. As noted above, the pattern of T_1 decrease that is observed as a function of imbibition and through CRAMPS detection parallels the pattern observed for the water protons observed through SP/MAS detection. It is proposed here that water entering the barley grain during imbibition provides a "T_1 reservoir" that is available for other protons contained within the grain by means of dipolar-mediated spin–spin flip-flops between the protons in more mobile structures and protons contained in the more rigid, but hydrated, grain components. This hypothesis is consistent with the observed difference in CRAMPS-detected proton T_1 values between grains imbibed to similar hydration levels in D_2O and H_2O. The observed T_1 difference between H_2O-imbibed and D_2O-imbibed grains may be due to a relaxation sink that mobile H_2O protons provide in H_2O-imbibed grains that is largely missing in D_2O-imbibed grains.

Most of the decreases in the water proton T_1 values observed in the CRAMPS or MAS-only approaches, and thus the largest decrease in motional correlation time (τ), is seen during the very early stage of imbibition, between the state of quiescence and imbibition to a water content of 15%. This early stage of imbibition is characterized by a rapid influx of water, presumably accompanied by filling of the strongest hydration sites in the seed, i.e., polar surfaces of macromolecules (Chung and Pfost, 1967; Vertucci and Leopold, 1984). The saturation (or complete filling) of the strong hydration sites by water in seeds varies with the species, and even within a species it varies with the composition of the seed. Nevertheless, a barley grain that was imbibed to a water content of 15% in this study is in the region of water content previously characterized (Chung and Pfost, 1967; Rockland, 1969; Vertucci and Leopold, 1984) for the appearance of "free" water in seeds. Therefore, it is proposed here that the steep drop in proton T_1 values during the initial stage of imbibition, up to a water content of 15%, corresponds to the filling of the strong hydration sites. After that initial imbibitional stage, the measured proton T_1 values level off, decreasing only slightly over the remaining course of germination. For the bulk of the protons in the grains, including the newly entering water protons, motion with $\tau_c \sim \omega_o^{-1}$ may not increase substantially after the initial phase of imbibition characterized by the steep decline in T_1.

Lipid protons contribute to the proton CRAMPS spectrum of a barley grain. Yet MAS-only detected proton T_1 values for the lipid peaks do not follow the biphasic pattern of sharp proton T_1 decline followed by modest proton T_1 decline over the course of imbibition in the same way that water proton T_1 values observed by CRAMPS and MAS-only techniques decrease with imbibition. This difference between the CRAMPS-detected grain proton T_1 and MAS-only detected lipid-proton T_1 behaviors can be explained. First, the barley-grain proton CRAMPS spectra, and hence the CRAMPS-detected T_1 values, are dominated by carbohydrate protons and, at later stages of imbibition, by water protons. Therefore, the lipid–proton spin-lattice relaxation behavior contributes very little to the CRAMPS-detected proton T_1 values measured for the barley grains. Second, lipids are highly mobile molecules and as such do not manifest strong internuclear proton–proton dipolar couplings. The spin–spin flip-flop mechanism that can provide proton T_1 averaging in solids is thus attenuated in lipids, so it is not necessarily expected that mobile lipids will have proton T_1 values comparable with those of the surrounding solid matrix. Nor is it expected that water protons will act as a "T_1 reservoir" for lipid protons. Hence, proton T_1 values measured for lipids in imbibed barley grains do not follow the same pattern as that observed for water and macromolecular protons.

The dephasing results obtained on all the grains reveal distinctly different components that can be qualitatively associated with different regimes of mobilities. As mentioned above, the Gaussian decay components arise from protons confined to rigid regions of the grain. The Lorentzian nature of dephasing decay for some protons indicates that the dipole–dipole interaction for those protons experiences a substantial degree of averaging during the dephasing period; this average can be the result of motion and/or spin exchange (Anderson and Weiss, 1953; Abragam, 1961; Jurkiewicz et al., 1989). Lorentzian time constants for transverse magnetization decay reported herein fall into three classifications: fast (10^{-2} ms), intermediate (10^{-1} to 10^{0} ms), and slow (10^{2} ms). Only the slow Lorentzian decays are consistent with the rapid motional narrowing of liquids. The fast and intermediate Lorentzian decays are indicative of exchange and/or motional regimes sufficiently fast and random *partially* to average the proton–proton rigid-lattice dipolar interaction that is typically tens of kilohertz in magnitude. The fast Lorentzian decays, although they indicate some motional averaging, are characterized by time constants that are similar to those of the Gaussian decays and therefore suggest a motional regime similar to that of a nearly rigid environment. Nevertheless, the observed

Lorentzian decay components all correspond to those protons that experience *some* motional freedom and/or exchange.

Gaussian decay components observed by CRAMPS detection for the 1.3-, 3.7-, and 4.9-ppm peaks of the barley grain spectra are characteristic of the protons of starch and protein macromolecules. When the barley grain has been imbibed to a water content of 24%, this fast decay component changes from Gaussian to Lorentzian in decay behavior and in general remains Lorentzian for the rest of the imbibition period, up to germination. This shift from Gaussian to fast Lorentzian decay indicates that the correlation time characterizing the motion and/or exchange in the system is sufficiently small that averaging of the dipolar perturbation to the proton linewidth can be exerted (Anderson and Weiss, 1953; Abragam, 1961; Jurkiewicz et al., 1989). However, because the dephasing decay time constant remains small, the correlation time for the completion of a random rotation must be relatively large compared with the correlation times describing intermediate and slow Lorentzian decays. A possible physical explanation for the switch from Gaussian to fast Lorentzian decay is that hydration becomes sufficient to provide motional freedom to the macromolecular lattices. The 3.7-ppm peak of the ^{1}H CRAMPS barley-grain spectrum contains a Gaussian-decay component up to a hydration level of 21%. The Gaussian component appears to become Lorentzian for a hydration level of 29%, then appears to switch back to Gaussian for a hydration level of 34%, and then apparently goes back to Lorentzian at germination (hydration level 34%). This *apparent* flip-flop between Gaussian and Lorentzian behaviors may be an anomaly that could result from the technical difficulties associated with the dephasing measurements.

Protons contributing to the 1.3-ppm peak in the CRAMPS spectra are protein protons, and methyl and methylene protons of lipids. The lipid protons maintain a slow Lorentzian decay in the grains, from quiescence to germination. Because of the higher degree of chemical shift resolution in MAS-only experiments, lipid proton decay rates observed by MAS-only detection are more specific for particular lipid-chain sites than are the CRAMPS data. Only the 1.3-ppm peak in the MAS-only spectra, representing methylene protons, contains just a slow Lorentzian decay component. All the other lipid peaks from the MAS-only spectra also contain an intermediate Lorentzian decay component. This intermediate component is characteristic of structures with hindered motion, relative to the slow Lorentzian component. In barley grains ~33% of the lipid component is phospholipid and glycolipid, which are located mainly in membrane bilayers (Price and Parsons, 1979). The current model of lipid bilayer packing places the portion of the methylene chain closest to the head group in the *trans* conformation, with adjacent chains packing closely together (Voet and Voet, 1990). The double bonds in the unsaturated lipids (which are almost exclusively *cis*) disrupt this close chain packing and provide the "hinge point" for the distal portion of the methylene chain, which is free to move rapidly and randomly and intertwine with methylene chains from lipid molecules that have their polar head groups on the other side of the bilayer. The highly motional regions of lipid chains near the double-bond sites essentially constitute "hinges" in this model. The site of unsaturation itself is the interface between the random and close-packed regions of lipid chains. The relatively high ratio of intermediate-to-slow decay components for the 5.3-ppm vinyl protons may provide support for this model of lipid membranes that places the lipid double bonds at "hinge points" in the chain. Perhaps some lipid-chain vinyl groups are more closely associated with the randomly packed portion of the bilayer, whereas other vinyl groups are more closely associated with the packed region of the bilayer.

According to this model of lipid bilayers, and the explanation of dephasing time constants given above, one would expect an intermediate decay rate for the lipid-chain methylene protons corresponding to the "packed" region of the bilayer. If neighboring lipid chains in the packed regions jump rapidly in concerted motion between two or more *trans* orientations and the chains expand and contract rapidly along the chain axis to approximate rapid isotropic motion, then only a large Lorentzian time constant (slow decay) would be observed. Regardless of the exact nature of the motions experienced by the lipid methylene chains, it must include fast, random, large-amplitude motions to produce only a slow Lorentzian transverse magnetization decay for those protons.

As observed for the 5.3-ppm protons, the 2.0-ppm allyl protons exhibit biphasic transverse decay behavior, but the ratio of intermediate-to-slow decay contributions is less than that for the 5.3-ppm protons. As mentioned above, the faster-decaying Lorentzian component observed for the 5.3-ppm protons may be influenced by the overlapping water peak, and therefore the significance of the ratio of intermediate-to-slow decay contributions in the 5.3-ppm peak is questionable at this time. However, the majority of the allyl protons at 2.0 ppm are characterized by the slowly decaying Lorentzian component, corresponding to the more highly mobile environment. Methyl protons at 0.8 ppm in the MAS-only spectra also display restricted motional behavior in that an intermediate Lorentzian decay component is observed for these protons in all the grains studied. Perhaps the faster decay component corresponds to those methyl groups in the lipid that are associated with membrane-embedded proteins. Proteins may constitute up to 50% of a lipid-bilayer structure (Voet and Voet, 1990) and as such could have a substantial effect on the motional freedom of nearby lipid chains. If the lipid chains conform to the shape of the protein, then a lipid-chain methyl group may become temporarily "stuck" in a cleft or other protein surface feature that restricts the motion of that methyl group. The intermediate Lorentzian decay component of the vinyl and allyl protons may also be explained by restricted motion of the lipids near proteins. Once again, the lack of an intermediate decay constant for lipid methylene protons indicates that motion in those portions of the lipid chains must not be significantly hindered.

A popular hypothesis of seed hydration proposes that membranes undergo phase transitions from a hexagonal phase, which is stable at low levels of hydration, to a membrane lamellar phase at higher levels of hydration (Simon, 1974). However, x-ray data collected on model seed membrane systems (McKersie and Stinson, 1980) and the NMR data presented here on quiescent and imbibed barley grains show no evidence of this proposed phase change. As mentioned above, membrane lipid is a significant fraction of the total lipid in barley grains. Changes in the structure and dynamics of membrane bilayers should affect the NMR parameters of the lipids to some extent. Phase changes in chemical systems typically induce large (often abrupt) changes in the observed NMR relaxation constants, T_1 and T_2, but the relaxation times observed for lipids in the grains studied here do not show large changes with imbibition time. In fact, the T_1 and large Lorentzian T_2 constants measured for the lipid protons are relatively constant over the course of imbibition.

The slowly dephasing component observed for the 4.9-ppm peak by CRAMPS progresses from an intermediate to a slow Lorentzian decay component during barley grain imbibition. This component of the 4.9-ppm peak is assigned to water protons at the onset of germination and, as hydration progresses, is assigned to water protons and the protons from other molecules that are in rapid exchange with water protons. At the point of germination (corresponding to 34% water), the decay constant of 7.4 ms for the 4.9-ppm peak is characteristic of liquidlike protons (Aksenov et al., 1982) but still remains small compared with the decay constant of ~14 ms for water protons of the highest mobility that have been observed in seeds (Aksenov et al., 1982). It is possible that interference between the motional time dependence of highly mobile water and the CRAMPS multiple-pulse cycle interferes with observation of the highly mobile water.

When the frequency of motion of a proton-containing species is equal to or comparable with the MP cycle time, the averaging of the proton dipolar interaction by the MP cycle is disrupted, because the dipolar Hamiltonian changes during the MP attempt to average it (Wittebort et al., 1988). This disruption of the dipolar averaging by motion can yield peaks in the CRAMPS spectrum that are artificially broad or can even escape detection because of the large residual linewidth that can arise from the incomplete dipolar averaging. Some of the water present in the imbibed barley grains may then escape detection by CRAMPS, thereby not contributing a slow Lorentzian decay component to the CRAMPS-detected water peak. SP/MAS techniques do not include a dipolar-averaging MP sequence, and so detection by MAS-only does not miss fast-motion components unless the MAS rotor cycle time is comparable with the motional τ_c. A slow Lorentzian component in the water peak, indicative of highly mobile water, is observed by MAS-only detection for the germinated grain, with a T_2 value of 11 ms. The intermediate Lorentzian decay component observed as part of the water peak by CRAMPS and MAS-only detection corresponds to the waters of hydration in the grain (Aksenov et al., 1982).

Phase changes in lipid membranes (McKersie et al., 1988) and lipid structural changes, including hydrolysis of lipids (Wilson and McDonald, 1986; McKersie et al., 1988; Stefanov et al., 1988) and oxidation of unsaturated lipids (Harman and Mattick, 1976; Stefanov et al., 1988) are often invoked as possible causes of, or often correlated with, a loss of seed viability during aging. Especially susceptible to lipid damage are the membranes of the embryo, for which successful reestablishment of metabolism and growth are essential for germination. Although the M-W-26 grains show a total loss of viability, the NMR results presented here show that the lipids of the M-W-26 grains are comparable with those lipids of the untreated and M-D-26 grains in terms of SP/MAS spectral features and T_2 values. The only noticeable difference between the proton NMR behavior of the lipid protons of the M-W-26 grain and that of the untreated grains is the consistently smaller T_2 value for the methylene protons of the M-W-26 grain relative to the methylene proton T_2 value of the untreated grains, when observed by MAS-only detection. The relatively small T_2 value for the methylene protons of the M-W-26 grain may be indicative of a loss of fluidity in the lipid membranes. However, T_2 results obtained on the excised barley-grain embryos reveal no evidence of lipid alteration during aging.

The lipid content of some species of seeds does not change during aging, but it does in others (Perlet al., 1987). It has been proposed that lipid oxidation occurs to a significant extent in seeds only during aging under dry conditions, whereas denaturation of proteins is responsible for increases in membrane permeability during aging under conditions of higher relative humidity (Harrington, 1973). It would be interesting to investigate, by ^1H relaxation studies of the type performed here, lipid dynamics in those seed species that are known to suffer from lipid degradation during loss of seed viability to determine whether ^1H NMR is a sensitive measure of these changes.

Structural alteration of lipids in seeds because of hydrolysis of phospholipids and triglycerides may be more difficult to observe than saturation of double bonds by these NMR techniques. The relative ratios of the lipid proton resonances would not change substantially with hydrolysis. It has been shown that the temperature of the crystalline/gel-phase transition is altered by elevated levels of free fatty acids in lipid membranes (McKersie et al., 1988). Variable-temperature NMR results would be useful to probe the temperature dependence of this phase transition in aged seed tissues.

CONCLUSIONS

Solid-state ^1H NMR experiments are useful tools for probing the dynamics and structure of intact barley

grains. Relaxation parameters of imbibing grains can be assigned qualitatively to motional regimes within the grains that are consistent with increasing levels of hydration during imbibition. These relaxation data have been used to design spin-exchange experiments for examining the progress of hydration in seeds, a subject to be treated in a later publication. The proton relaxation behavior characterized in the study reported here can also be used as the basis for designing ^{1}H NMR imaging strategies for the study of seed germination; such studies have been initiated in this laboratory.

The barley grains used in this study do not exhibit signs of extensive lipid membrane or storage-lipid degradation during loss of viability. Lipid degradation in these grains may occur to a limited extent, but the mechanism for aging most likely involves other factors.

The authors gratefully acknowledge the partial support of this research by the Coors Brewing Company and the helpful discussions and assistance of Dr. Sharon Sowa and Dr. Christina Vertucci of the U.S.Department of Agriculture's National Seed Storage Laboratory at Colorado State University.

REFERENCES

Abragam, A. 1961. Principles of Nuclear Magnetism. Clarendon Press, Oxford.

Aksenov, S. I., N. A. Askochenskaya, and E. A. Golovina. 1982. Investigation of initial steps of swelling of wheat seeds by NMR spin echo technique. *Dokl. Biophys.* 262/264:86–89.

Anderson, P. W., and P. R. Weiss. 1953. Exchange narrowing in paramagnetic resonance. *Rev. Mod. Phys.* 25:269–276.

Andrew, E. R., L. F. Farnell, M. Firth, T. D. Gledhill, and I. Roberts. 1969. High-speed rotors for nuclear magnetic resonance studies on solids. *J. Magn. Reson.* 1:27–34.

Bewley, J. D., and M. Black. 1985. Seeds: Physiology of Development and Germination. Plenum Press, New York. 11.

Bloembergen, N., E. M. Purcell, and E. V. Pound. 1948. Relaxation effects in nuclear magnetic resonance absorption. *Phys. Rev.* 73:679–712.

Bovey, F. A. 1988. Nuclear Magnetic Resonance Spectroscopy, 2nd ed. Academic Press, New York.

Bovey, F. A., L. Jelinski, and P. A. Mirau. 1987. Nuclear Magnetic Resonance Spectroscopy, 2nd ed. Academic Press, New York.

Bronnimann, C. E., B. L. Hawkins, M. Zhang, and G. E. Maciel. 1988. Combined rotation and multiple pulse spectroscopy as an analytical proton nuclear magnetic resonance technique for solids. *Anal. Chem.* 60:1743–1750.

Bronnimann, C. E., R. C. Zeigler, and G. E. Maciel. 1988. Proton NMR study of dehydration of the silica gel surface. *J. Am. Chem. Soc.* 110:2023–2026.

Burum, D. P., and W. K. Rhim. 1979. Analysis of multiple pulse NMR in solids. *J. Chem. Phys.* 71:944–956.

Chen, S-C., R. M. Elofson, and J. M. MacTaggart. 1979. Carbon-13 nuclear magnetic resonance studies of lipids and starch digestion in intact seeds. *J. Agric. Food Chem.* 27:435–438.

Chung, D. S., and H. B. Pfost. 1967. Adsorption and desorption of water vapor by cereal grains and their products. I: Heat and free energy changes of adsorption and desorption. *Trans. Am. Soc. Agric. Eng.* 10:549–551, 555.

Colnago, L. A., and P. R. Seidl. 1983. Application of carbon-13 nuclear magnetic resonance to the germination of soybean seeds in vivo. *J. Agric. Food Chem.* 31:459–461.

Conway, T. F., and L. F. Johnson. 1969. Nuclear magnetic resonance measurement of oil "unsaturation" in single viable corn kernels. *Science* 164:827–828.

Conway, T. F., and R. J. Smith. 1962. Determination of fat in corn and corn germ by wide-line nuclear magnetic resonance (NMR) techniques. *Devel. Appl. Spectrosc.* 2:115–127.

Derome, A. E. 1987. Modern NMR Techniques for Chemistry Research. Pergamon, New York.

Farrar, T. C., and E. D. Becker. 1971. Pulse and Fourier Transform NMR: Introduction to Theory and Methods. Academic Press, New York.

Freeman, R., and H. D. W. Hill. 1971. Fourier transform study of NMR spin-lattice relaxation by "progressive saturation". *J. Chem. Phys.* 54: 3367–3377.

Gerstein, B. C., C. Chou, R. G. Pembleton, and R. C. Wilson. 1977. Utility of pulse nuclear magnetic resonance in studying protons in coal. *J. Phys. Chem.* 81:565–570.

Hahn, E. L. 1950. Spin echoes. *Phys. Rev.* 80:580–594.

Harman, G. E., and L. R. Mattick. 1976. Association of lipid oxidation with seed ageing and death. *Nature (London).* 206:323–324.

Harrington, J. F. 1973. Biochemical basis of seed longevity. *Seed Sci. Technol.* 1:453–461.

Haw, J. F., and G. E. Maciel. 1983. Carbon-13 nuclear magnetic resonance spectrometry of oil seeds with cross polarization and magic-angle spinning. *Anal. Chem.* 55:1262–1267.

International Seed Testing Association. 1976. International rules for seed testing. *Seed Sci. Technol.* 4:1–177.

Jurkiewicz, A., C. E. Bronnimann, and G. E. Maciel. 1989. ^{1}H CRAMPS n.m.r. study of the molecular-macromolecular structure of coal. *Fuel.* 68:872–876.

Jurkiewicz, A., C. E. Bronnimann, and G. E. Maciel. 1990. ^{1}H CRAMPS studies of molecular dynamics of a premium coal. *Fuel.* 69:804–809.

Kessemeier, H., and R. E. Norberg. 1967. Pulsed nuclear magnetic resonance in rotating solids. *Phys. Rev.* 155:321–337.

Kuntz, I. D., and W. Kauzmann. 1974. Hydration of proteins and polypeptides. *Adv. Protein Chem.* 28:239–345.

Lowe, I. J. 1959. Free induction decay of rotating solids. *Phys. Rev. Lett.* 2:285–287.

Maciel, G. E., C. E. Bronnimann, and B. L. Hawkins. 1990. High-resolution ^{1}H nuclear magnetic resonance in solids via CRAMPS. *In* Advances in Magnetic Resonance: The Waugh Symposium, Vol. 14. W. S. Warren, editor. Academic Press, San Diego. 125–150.

McKersie, B. D., and R. H. Stinson. 1980. Effect of dehydration on leakage and membrane structure in *Lotus corniculatus* L. seeds. *Plant Physiol.* 66:316–320.

McKersie, B. D., T. Senaratna, and J. F. Gusse. 1988. Age-induced changes in cellular membranes of imbibed soybean seed axes. *Physiol. Plant.* 73:85–91.

O'Donnell, D. J., J. J. Ackermann, and G. E. Maciel. 1981. Comparative study of whole seed protein and starch content via cross polarization–magic angle spinning carbon-13 nuclear magnetic resonance spectroscopy. *J. Agric. Food Chem.* 29:514–518.

Perl, J., Y. Zohara, and Z. Feder. 1987. The effect of natural and accelerated aging on the lipid content and the fatty acid composition of seeds. *Acta Hort.* 215:61–67.

Price, P. B., and J. Parsons. 1979. Distribution of lipids in embryonic axis, bran-endosperm and hull fractions of hulless barley and hulless oat grain. *J. Agric. Food Chem.* 27:813–815.

Priestley, D. A. 1986. Seed Aging. Cornell University Press, Ithaca, New York.

Ridenour, C. F., and G. E. Maciel, 1995. "Investigation of barley grain imbibition via nuclear magnetic resonance, using ^{1}H-^{1}H spin exchange," *Biophys. J.* (submitted).

Rockland, L. B. 1969. Water activity and storage stability. *Food Technol.* 23:1241–1251.

Rutar, V. 1989. Magic angle sample spinning nmr spectroscopy of liquids as a nondestructive method for studies of plant seeds. *J. Agric. Food Chem.* 37:67–70.

Schaefer, J., and E. O. Stejskal. 1974. Determination of oil, starch, and protein content of viable intact seeds by carbon-13 nuclear magnetic resonance. *J. Am. Oil Chem. Soc.* 51:562–563.

Seewaldt, V., D. A. Priestley, A. C. Leopold, G. W. Feigenson, and F. Goodsaid- Zalduondo. 1981. Membrane organization in soybean seeds during hydration. *Planta.* 152:19–23.

Simon, E. W. 1974. Phospholipids and plant membrane permeability. *New. Phytol.* 73:377- 420.

Stefanov, K. L., N. V. Yanishlieva, Z. V. Zhukov, V. D. Tsydendambaev, V. P. Pchelkin, and A. G. Vereshchagin. 1988. Influence of accelerated aging on the content and fatty acid composition of free and bound lipids in sunflower seeds. *Appl. Biochem. Microbiol.* 23:406–411.

Tomassetti, M., L. Campanella, and M. Delfini. 1986. Determination of water in plant samples: a comparative thermogravimetric and NMR study on different species of seeds. *Thermochim. Acta.* 105:179–190.

Vertucci, C. W., and A. C. Leopold. 1984. Bound water in soybean seed and its relation to respiration and imbibitional damage. *Plant Physiol.* 75: 114–117.

Voet, D., and J. G. Voet. 1990. Biochemistry. John Wiley & Sons, New York. 282–291.

Wilson, D. O., Jr., and M. B. McDonald, Jr. 1986. The lipid peroxidation model of seed ageing. *Seed Sci. Technol.* 14:269–300.

Wittebort, R. J., M. G. Usha, D. J. Ruben, D. E. Wemmer, and A. Pines. 1988. Observation of molecular reorientation in ice by proton and deuterium magnetic resonance. *J. Am. Chem. Soc.* 110: 5668–5671.